© 2021. Published by The Company of Biologists Ltd | Journal of Cell Science (2021) 134, jcs258341. doi:10.1242/jcs.258341

RESEARCH ARTICLE

Spatiotemporal control of pathway sensors and cross-pathway feedback regulate a differentiation MAPK pathway in yeast

Aditi Prabhakar*, Beatriz González, Heather Dionne‡, Sukanya Basu§ and Paul J. Cullen¶

ABSTRACT

Mitogen-activated protein kinase (MAPK) pathways control cell differentiation and the response to stress. In *Saccharomyces cerevisiae*, the MAPK pathway that controls filamentous growth (fMAPK) shares components with the pathway that regulates the response to osmotic stress (HOG). Here, we show that the two pathways exhibit different patterns of activity throughout the cell cycle. The different patterns resulted from different expression profiles of genes encoding mucin sensors that regulate the pathways. Cross-pathway regulation from the fMAPK pathway stimulated the HOG pathway, presumably to modulate fMAPK pathway activity. We also show that the shared tetraspan protein Sho1p, which has a dynamic localization pattern throughout the cell cycle, induced the fMAPK pathway at the mother-bud neck. A Sho1p-interacting protein, Hof1p, which also localizes to the mother-bud neck and regulates cytokinesis, also regulated the fMAPK pathway. Therefore, spatial and temporal regulation of pathway sensors, and cross-pathway regulation, control a MAPK pathway that regulates cell differentiation in yeast.

KEY WORDS: Mucins, Cell cycle, Mother-bud neck, Septins, MAPK, Cell synchronization

INTRODUCTION

Mitogen-activated protein kinase (MAPK) pathways control growth (Johnson and Lapadat, 2002; Lavoie et al., 2020), cell differentiation (Chen and Thorner, 2007; Raman et al., 2007; Dinsmore and Soriano, 2018) and the response to stress (Roux and Blenis, 2004; Yoon and Seger, 2006; Shaul and Seger, 2007; Papa et al., 2019). MAPK pathways can operate in interconnected networks where inputs from multiple pathways converge (Jordan et al., 2000; Fischer et al., 2018). Mis-regulation of MAPK pathways is linked to many diseases (Lee et al., 2000; Hirosumi et al., 2002; Maekawa et al., 2005; Omori et al., 2006; Rodriguez-Viciana et al., 2006; Roberts and Der, 2007; Lawrence et al., 2008). Therefore, understanding how MAPK pathways induce a specific signal in an integrated network remains an important question.

In the budding yeast *Saccharomyces cerevisiae*, MAPK pathways control cell differentiation in response to extrinsic cues. In response to nutrient limitation, yeast and other fungal species can undergo filamentous/invasive/pseudohyphal growth, where cells differentiate into filamentous cells (Gimeno et al., 1992; Roberts and Fink, 1994; Mosch et al., 1996; Peter et al., 1996; Leberer et al., 1997; Pan et al., 2000; Gancedo, 2001; Adhikari et al., 2015b). In some fungal pathogens, filamentous growth is crucial for virulence (Lo et al., 1997). In yeast, the MAPK pathway that regulates filamentous growth (Fig. 1A, fMAPK, green) is controlled by the mucin glycoprotein Msb2p (Cullen et al., 2004). Msb2p functions with a four-pass (tetraspan) adaptor protein, Sho1p (O'Rourke and Herskowitz, 1998; Cullen et al., 2004), to regulate the Rho GTPase Cdc42p, which, when activated, binds to the p21-activated (PAK) kinase Ste20p (Peter et al., 1996; Leberer et al., 1997; Johnson, 1999; Bi and Park, 2012). Ste20p regulates the MAPK cascade composed of the MAP kinase kinase kinase (MAPKKK) Ste11p, which phosphorylates and activates the MAP kinase kinase (MAPKK) Ste7p, which in turn phosphorylates and activates the MAP kinase Kss1p (Roberts and Fink, 1994; Madhani et al., 1997). Active Kss1p regulates the transcription factors Ste12p and Tec1p, which induce target gene expression to regulate differentiation to the filamentous cell type (Ma et al., 1995; Madhani and Fink, 1997; Bardwell et al., 1998; Rupp et al., 1999; Roberts et al., 2000; van der Felden et al., 2014; Pelet, 2017).

Some proteins that regulate the fMAPK pathway also regulate other MAPK pathways, including the HOG (O'Rourke and Herskowitz, 2002; Cullen et al., 2004; Tatebayashi et al., 2006) and mating pathways (Sabbagh et al., 2001; Breitkreutz and Tyers, 2002; Bardwell, 2004; Schwartz and Madhani, 2004; Bardwell, 2006). The HOG pathway responds to changes in osmolarity and is composed of partially redundant branches (Fig. 1A; Tatebayashi et al., 2006). In the Ste11p branch of the HOG pathway, Ste11p phosphorylates the MAPKK Pbs2p (Brewster et al., 1993; Maeda et al., 1994). Different mucin sensors regulate the two pathways. Hkr1p regulates the HOG pathway, while Msb2p regulates the fMAPK and HOG pathways (Fig. 1A; O'Rourke and Herskowitz, 2002; Cullen et al., 2004; Tatebayashi et al., 2007; Yamamoto et al., 2016). Msb2p and Hkr1p regulate the HOG pathway by different mechanisms (Tanaka et al., 2014). Importantly, Hkr1p does not regulate the fMAPK pathway, and overexpression of the mucins induces different target genes (Pitoniak et al., 2009). The two pathways also function in an antagonistic manner (Davenport et al., 1999; Adhikari and Cullen, 2014). Although selectivity in propagating a downstream signal presumably occurs at the level of the mucins and adaptors, how this occurs is not well understood.

The HOG pathway can be activated at any stage of the cell cycle (Nagiec and Dohlman, 2012), although it preferentially induces cell-cycle arrest in G1 (Escoté et al., 2004). We previously found that the activity of the fMAPK pathway fluctuates throughout the cell cycle (Prabhakar et al., 2020), and we show here that the fMAPK and the HOG pathways show different patterns of cell-cycle regulation, which results from different gene expression profiles of

Department of Biological Sciences, University at Buffalo, Buffalo, NY 14260-1300, USA.
*Present address: Department of Molecular Metabolism, Harvard T.H. Chan School of Public Health, Boston, MA 02115, USA. ‡Present address: Howard Hughes Medical Institute Janelia Farm Research Campus, Ashburn, VA 20147, USA. §Present address: Department of Pharmacology & Therapeutics, Roswell Park Comprehensive Cancer Center, Buffalo, NY 14263, USA.

¶Author for correspondence (pjcullen@buffalo.edu)

P.J.C., 0000-0002-6703-1480

Handling Editor: David Glover
Received 23 December 2020; Accepted 21 June 2021

Journal of Cell Science (2021) 134, jcs258341. doi:10.1242/jcs.258341

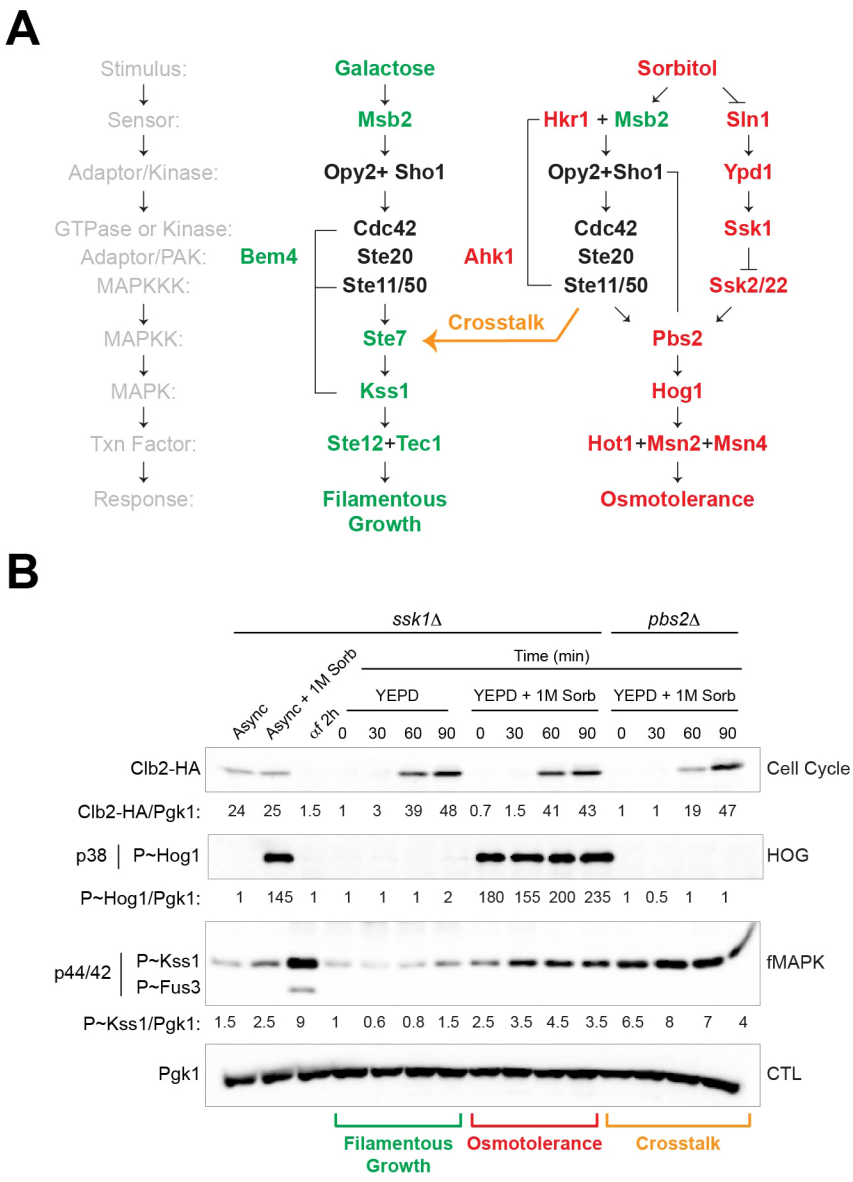

Fig. 1. Cdc42p-dependent pathways in yeast share components yet induce different responses. (A) MAPK pathways that regulate filamentous growth (green, fMAPK) and osmolarity (red, HOG). Proteins shown in black regulate both pathways. Black lines indicate interactions between adaptors and core pathway regulators. Orange arrow indicates crosstalk between the HOG and the fMAPK pathway, which occurs in cells lacking Pbs2p or Hog1p. (B) Immunoblots of *ssk1*Δ (PC7494) and *pbs2*Δ (PC7493) mutants synchronized in G1. For the *ssk1*Δ mutant, synchronized cells were released into YEPD medium, and samples were harvested at the indicated times to measure basal HOG levels. Another aliquot was harvested and resuspended in YEPD supplemented with 1 M sorbitol (YEPD+1 M Sorb) for 5 min before harvesting to measure activated HOG levels. Samples were also harvested before (Async) and during α factor treatment (αf 2 h). A sample of asynchronous culture was harvested and resuspended in YEPD supplemented with 1 M sorbitol for 5 min (Async+1 M Sorb). For the *pbs2*Δ mutant, synchronized cells were released into YEPD medium and at indicated times, resuspended in YEPD+1 M Sorb for 5 min before harvesting. Ratios of Clb2p-HA to Pgk1p, P~Kss1p to Pgk1p, and P~Hog1p to Pgk1p relative to time 0 (set to 1) are shown.

the mucin sensors. We also show that activation of the fMAPK pathway induces the HOG pathway, generating cross-pathway regulation between the pathways. We also show that the level of Sho1p is cell-cycle regulated, and that Sho1p and the cytokinesis regulator Hof1p regulate the fMAPK pathway at the mother-bud neck. Collectively, our findings bring to light pathway-specific regulatory aspects of a differentiation-type MAPK pathway. The activity of many signaling pathways may be regulated by the cell cycle and subject to precise spatial control by their cognate sensors.

RESULTS

MAPK pathways that share components show different patterns of activity throughout the cell cycle

To investigate the activity of the fMAPK pathway throughout the cell cycle, cells were synchronized using α factor, which arrests cells in the G1 phase of the cell cycle (Elion et al., 1993; Peter et al., 1993; Peter and Herskowitz, 1994). Synchronized cells showed low levels of phosphorylated Kss1p (P~Kss1p) early in the cell cycle (Fig. S1A, P~Kss1, 0 min to 80 min). When levels of the mitotic cyclin Clb2p-Myc dropped in M phase (Richardson et al., 1992; Eluère et al., 2007; Kuczera et al., 2010; Cepeda-García, 2017), P~Kss1p levels increased (Fig. S1A, 100 min). Although the cell synchronization was less evident in the second cycle (based on Clb2p-Myc levels), P~Kss1p levels decreased (140 min) and increased again (160 min), as cells progressed through the second cycle. P~Kss1p levels were higher in the second cycle, which may be due to the depletion of nutrients, which stimulates the fMAPK pathway. The cell-cycle pattern of the fMAPK pathway seen above may result from pheromone treatment. Release of cells from hydroxyurea (HU), which arrests cells in S phase (Slater, 1973, 1974; Koç et al., 2004), also showed an increase in P~Kss1p levels throughout the cell cycle (Fig. S1B). In this case, P~Kss1p levels increased prior to the disappearance of Clb2-Myc. Both experiments show that fMAPK pathway activity fluctuates throughout the cell cycle.

The fMAPK pathway shares components with the *STE11* branch of the HOG pathway (Fig. 1A). Measuring HOG pathway activity in cells lacking the redundant *SLN1* branch (*ssk1*Δ) provides a readout of the activity of shared components. To determine whether HOG pathway activity changes throughout the cell cycle, phosphorylation of the MAPK Hog1p was measured in cells lacking the Sln1p

Journal of Cell Science (2021) 134, jcs258341. doi:10.1242/jcs.258341

branch (Fig. 1B, *ssk1*Δ). As reported (Posas and Saito, 1997), asynchronous *ssk1*Δ cells exposed to 1 M sorbitol showed elevated P∼Hog1p levels (Fig. 1B, P∼Hog1, Async+1 M Sorb). Synchronized *ssk1*Δ cells exposed to 1 M sorbitol also showed elevated P∼Hog1p levels (Fig. 1B, P∼Hog1, YEPD+1 M Sorb). Basal P∼Hog1p levels differed from P∼Kss1p levels throughout the cell cycle (Fig. S1C). These results indicate that the HOG pathway can be activated at any point in the cell cycle.

Cells lacking an intact HOG pathway (*pbs2*Δ mutant) exposed to osmotic stress exhibit crosstalk to the mating (O'Rourke and Herskowitz, 1998) and fMAPK pathways (Fig. 1A, orange arrow; Pitoniak et al., 2009). The *pbs2*Δ mutant synchronized by α factor showed elevated P∼Kss1p levels in response to 1 M sorbitol in asynchronous (Fig. S1D) and synchronized cells in all stages of the cell cycle (Fig. 1B, P∼Kss1, *pbs2*Δ, YEPD+1 M Sorb). Thus, the cell-cycle regulation of the fMAPK pathway was lost in the *pbs2*Δ mutant. P∼Kss1p levels were also elevated in *PBS2*+ cells exposed to 1 M sorbitol (Fig. 1B, P∼Kss1, *ssk1*Δ, YEPD+1 M Sorb, 30-90 min but not 0 min), which might result from basal crosstalk (Hao et al., 2008). P∼Hog1p was not detected in the *pbs2*Δ mutant exposed to 1 M sorbitol, because Pbs2p is required to phosphorylate Hog1p. Therefore, during crosstalk, the fMAPK pathway can be activated at early stages in the cell cycle. One conclusion that can be drawn from this result is that shared components between HOG and fMAPK pathways can function at early stages in the cell cycle. Thus, a pathway-specific factor may control cell-cycle regulation of the fMAPK pathway.

Expression of the gene encoding the mucin sensor Msb2p is cell-cycle regulated

To define how fMAPK pathway activity is regulated throughout the cell cycle, genetic suppression analysis was performed. Genetic suppression analysis can order components in a pathway using gain- and loss-of-function alleles. Hyperactive versions of fMAPK pathway components Msb2p* [GFP-Msb2p (Adhikari et al., 2015b)], Sho1p^{P120L} (Vadaie et al., 2008) and Ste11p-4 (Stevenson et al., 1992) were examined for the ability to bypass the low levels of fMAPK pathway activity seen early in the cell cycle. Ste11p-4 bypassed the low levels of fMAPK pathway activity (Fig. 2A). Msb2p* and Sho1p^{P120L} showed a partial bypass (Fig. S2A-C). Therefore, cell-cycle regulation of the fMAPK pathway occurs before Ste11p and at the level of Msb2p and Sho1p. Consistent with the role of the fMAPK pathway in delaying cell-cycle progression in G1 (Loeb et al., 1999; Madhani et al., 1999) and G2/M (Ahn et al., 1999; Rua et al., 2001; Vandermeulen and Cullen, 2020), Ste11p-4 showed a delay in Clb2p-HA accumulation (Fig. 2A, compare wild type at 60 min with *STE11-4* at 60 min). Crosstalk induced a similar delay [Fig. 1B, compare Clb2-HA levels in wild type (*ssk1*Δ) and *pbs2*Δ at 60 and 90 min], indicating that the fMAPK pathway impacts cell-cycle progression in this setting.

fMAPK pathway activity might fluctuate if the levels of one or more components change throughout the cell cycle. Msb2p levels directly impact fMAPK pathway activity (Cullen et al., 2004) and drive induction of fMAPK pathway targets (Pitoniak et al., 2009). A functional Msb2p-HA protein, expressed under the control of its endogenous promoter at the *MSB2* locus, showed low levels early in the cell cycle that peaked later in the cell cycle (Fig. 2B, Msb2). Msb2p-HA levels showed a similar pattern in cells synchronized by HU (Fig. S1B). By comparison, the levels of the HOG pathway mucin Hkr1p (Tatebayashi et al., 2007; Yang et al., 2009), also expressed as a HA fusion from its endogenous promoter, did not increase throughout the cell cycle (Fig. 2B, Hkr1). Because both mucins contained the same epitope fusion (HA) internal to both proteins in their glycosylated extracellular domains, we assumed that the HA epitope might be similarly accessible in both proteins, which could allow their levels to be directly compared. Msb2p-HA levels were 15-fold higher than Hkr1p-HA levels in asynchronous (Fig. 2C, Async) and synchronized (Fig. 2C, 100 and 160 min) cultures. Comparative proteomic studies show a similar trend (Breker et al., 2013; Yofe et al., 2016). The relative abundance of the mucins, and their different patterns of cell-cycle regulation, might explain the differences in activities of the fMAPK and the HOG pathways.

The mRNA levels of *MSB2* and *HKR1* were also examined throughout the cell cycle. *MSB2* mRNA levels were low following release from α factor treatment and higher as cells progressed through the cell cycle (Fig. 2D, *MSB2*). By comparison, *HKR1* mRNA levels were high early in the cell cycle (Fig. 2D, *HKR1*) but did not otherwise fluctuate. Thus, *MSB2* and *HKR1* genes show different patterns of gene expression throughout the cell cycle. *MSB2* levels were also higher than *HKR1* levels based on the analysis of a previously published dataset that examined the levels of *MSB2-lacZ* and *HKR1-lacZ* fusions in asynchronous cells (Pitoniak et al., 2009).

Exploring basal and activated fMAPK pathway activity throughout the cell cycle

As Msb2p regulates the fMAPK pathway through positive feedback, Msb2p levels might precede, and therefore induce, P∼Kss1p levels at M/G1. Alternatively, *MSB2* expression might be induced as a result of P∼Kss1p induction. To distinguish between these possibilities, the levels of Msb2p-HA and P∼Kss1p were compared following release from α factor at short time intervals. Low levels of Msb2p-HA at the beginning of the cell cycle gradually peaked by 40-50 min (Fig. 3A, Msb2, 12-fold increase relative to t=0), which was coincident with a small increase in P∼Kss1p levels (Fig. 3A, P∼Kss1, 2-fold increase relative to t=0). Msb2p levels are known to directly regulate fMAPK activity (Cullen et al., 2004; Vadaie et al., 2008; Adhikari et al., 2015b). The fact that an increase in Msb2p levels at 40-50 min (G1/S boundary) did not significantly increase P∼Kss1p levels suggests that other forms of regulation prevent Kss1p activation at this stage, such as from Swi4p and Sho1p (see below). After a drop at 80 min, Msb2p-HA levels increased again to peak at 100 min (14-fold increase relative to t=0), when P∼Kss1p levels rose at M/G1 (4-fold increase relative to t=0). These fluctuations correlated with *MSB2* mRNA levels (see Fig. 2D). Thus, Msb2p protein levels fluctuate within a single cell cycle and their rise towards the end of the cell cycle, which correlated with the rise in P∼Kss1p levels.

Up to this point, fMAPK pathway activity was examined under basal conditions. The fMAPK pathway is induced by growth in the non-preferred carbon source galactose (YEP-GAL; Karunanithi and Cullen, 2012). Cells synchronized by α factor in YEPD and released into YEP-GAL medium (inducing conditions) showed a delay in P∼Kss1p accumulation, which indicates that the fMAPK pathway is cell-cycle regulated under inducing conditions (Fig. 3B), consistent with previous observations (Prabhakar et al., 2020). Msb2p-HA levels also accumulated in YEP-GAL media prior to the increase in P∼Kss1p levels (Fig. 3B). Thus, the increase in Msb2p levels precedes and might therefore contribute to accumulation of P∼Kss1p levels throughout the cell cycle.

Clb2p accumulation showed an extended delay in YEP-GAL (Fig. 3B, 180 min) compared with YEPD media (Fig. 3A, 60-80 min). This extended delay in cell-cycle progression might result from glucose repression that involves the transcriptional repression

Journal of Cell Science (2021) 134, jcs258341. doi:10.1242/jcs.258341

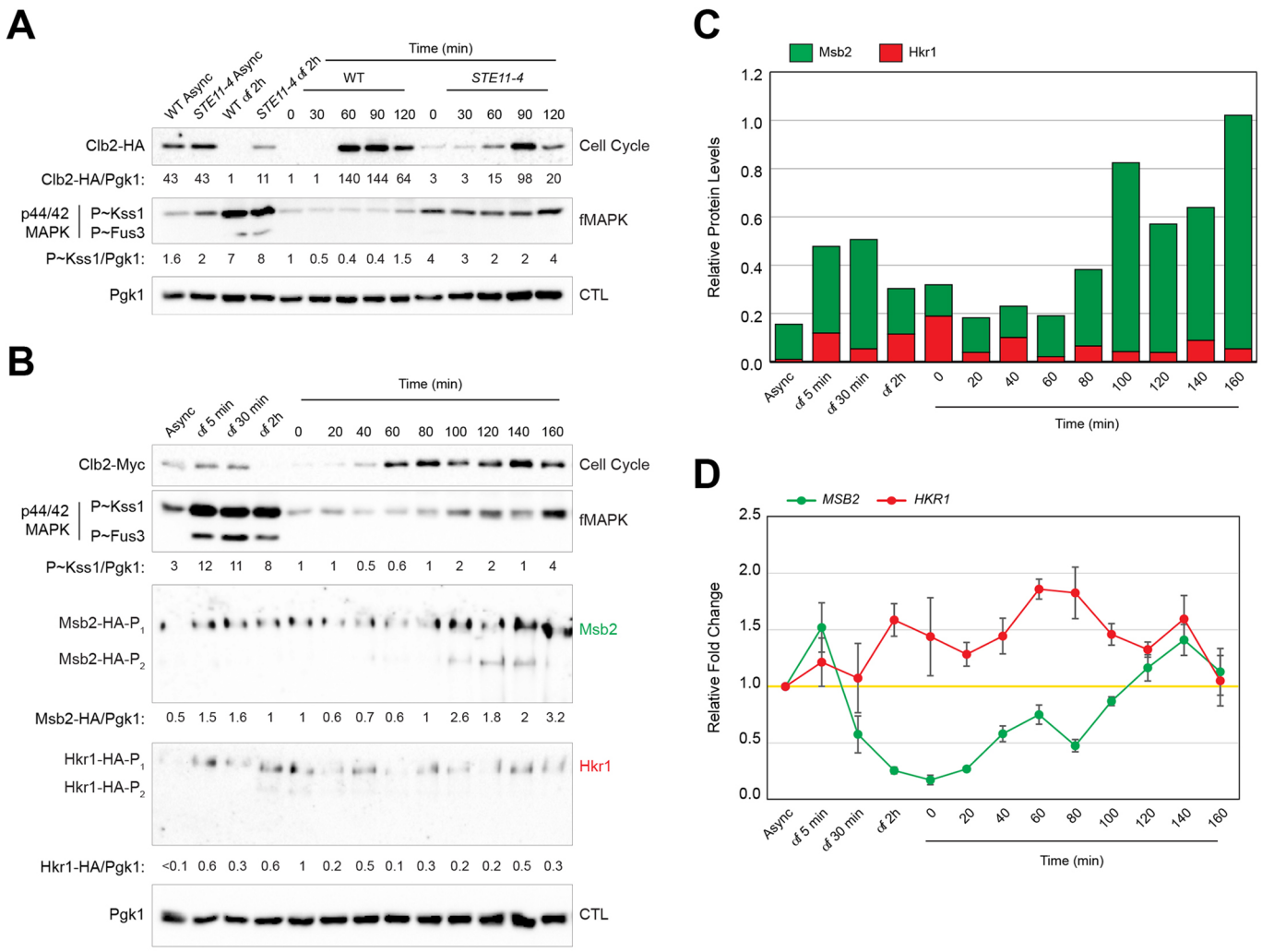

Fig. 2. Cell-cycle pattern of fMAPK activity corresponds to different expression patterns of the genes encoding the signaling mucins Msb2p and Hkr1p. (A) Immunoblots (IBs) of synchronized cultures of wild type (PC7492) and *STE11-4* strain (PC7492+p*STE11-4*) released into YEPD. See Fig. 1B for details. Ratios of P~Kss1p to Pgk1p relative to wild type at time 0 (set to 1) are shown. WT, wild type; CTL, loading control. (B) IBs of wild type containing Msb2p-HA (PC7495+p*STE4*) or Hkr1p-HA (PC7602+p*STE4*) synchronized in G1 and released into YEPD medium. Samples were harvested and probed as in Fig. 1B. Ratios of P~Kss1p to Pgk1p, Msb2p-HA to Pgk1p, and Hkr1p-HA to Pgk1p relative to time 0 (set to 1) are shown. (C) Quantitation of Msb2p-HA and Hkr1p-HA protein levels relative to Pgk1p from B. Green bar, Msb2p levels; red bar, Hkr1p levels. (D) RT-qPCR analysis of wild type (PC7602+p*STE4*) synchronized in G1 and released into YEPD medium. Fold changes in the mRNA levels of *MSB2* (green) and *HKR1* (red) at indicated time points relative to the asynchronous culture (Async). Yellow line, asynchronous levels. Data are mean±s.e.m. of four replicates: two biological replicates and two technical replicates. One-way ANOVA with Dunnett's test was used for statistical analysis. The fluctuations in *MSB2* mRNA levels were statistically significant at some timepoints (P<0.01). Specifically, αf=5 min, αf=2 h, t=0, t=20 min and t=80 min were different from other time points. The fluctuations in *HKR1* mRNA levels were not statistically significant (P=0.55).

of genes (*GAL* genes and many other genes) that metabolize non-preferred carbon sources (Carlson and Botstein, 1982; Nehlin et al., 1991; Wilson et al., 1996; De Vit et al., 1997). To examine fMAPK pathway activity in response to a sustained induction, cells pre-grown in YEP-GAL medium were synchronized and monitored. These cells also showed low levels of P~Kss1p after release from α factor (Fig. S3), but not the extended delay seen under pathway-inducing conditions. Thus, cell-cycle regulation of the fMAPK pathway is seen in basal, induced and sustained-inducing conditions.

In YEP-GAL medium, a new pattern of cell-cycle regulation was observed. Compared with basal conditions, where P~Kss1p levels peaked after Clb2p-HA levels fell (Fig. 3C, pink), under inducing conditions, P~Kss1p levels peaked at the same time as Clb2p-HA accumulation (Fig. 3C, blue). A similar trend was seen under sustained-inducing conditions (Fig. S3). P~Kss1p levels were 12-fold higher under inducing conditions than under basal conditions (Fig. 3C, compare left and right axes). The ability of the fMAPK pathway to partially bypass the cell-cycle regulation may result from GAL-dependent induction of the fMAPK pathway, which could occur through several mechanisms, including activation of the fMAPK pathway by glucose limitation through elevated processing of Msb2p (Vadaie et al., 2008).

Altering cell cycle regulation impacts fMAPK pathway activity and filamentous growth

Cell-cycle progression is regulated by transcription factors that include Swi4p/6p cell cycle box binding factor (SBF), which induces transcription of genes required for the progression from late G1 to S phase (Andrews and Herskowitz, 1989; Nasmyth and Dirick, 1991; Sidorova and Breeden, 1993). We tested whether altering cell-cycle progression, by loss of Swi4p and Swi6p, impacts fMAPK pathway activity and filamentous growth. We generated a

Journal of Cell Science (2021) 134, jcs258341. doi:10.1242/jcs.258341

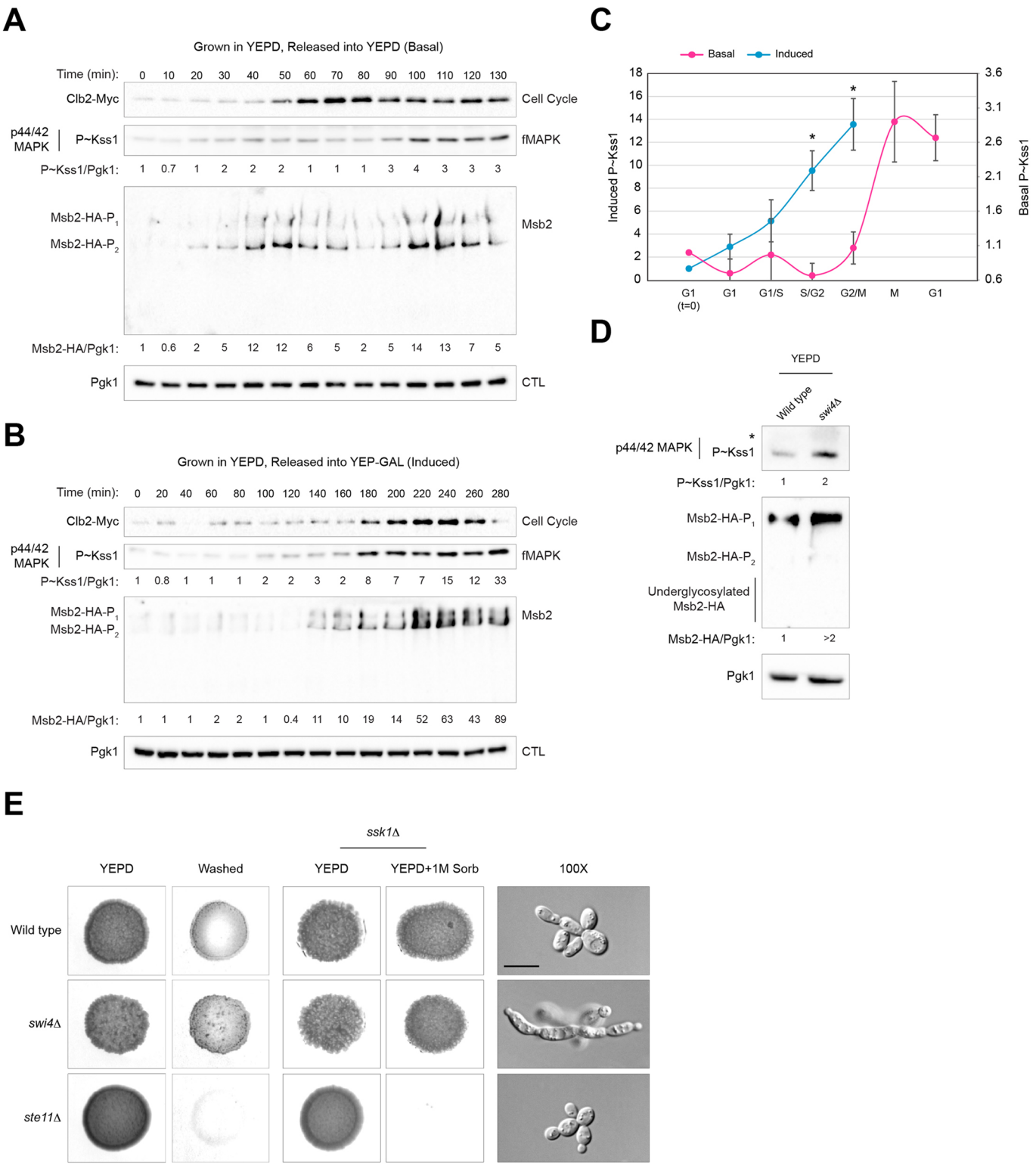

Fig. 3. See next page for legend.

*swi6*Δ mutant, which had a severe growth defect and was not tested further. We also generated a *swi4*Δ mutant, which had elevated levels of P~Kss1p and Msb2p-HA compared with wild type (Fig. 3D). Evaluation of the *swi4*Δ mutant by the plate washing assay (PWA), which measures invasive growth as a readout of fMAPK pathway activity (Roberts and Fink, 1994), showed hyper-invasive growth compared with wild type (Fig. 3E, washed). The *swi4*Δ mutant was not required for growth on high-osmolarity media, which may indicate that the protein does not regulate the HOG pathway (Fig. 3E, YEPD+1 M Sorb). The *swi4*Δ mutant also exhibited hyperpolarized growth (Fig. 3E, 100×), which may result from an extension of the G1 phase of the cell cycle (White et al.,

Journal of Cell Science (2021) 134, jcs258341. doi:10.1242/jcs.258341

Fig. 3. Cell-cycle regulation of the fMAPK pathway is impacted by the activation state of the pathway and the G1/S transcription factor Swi4p. (A) Immunoblots (IBs) of wild type containing Msb2p-HA (PC7495+p*STE4*) pre-grown and synchronized in YEPD and released into YEPD medium. Samples were harvested during the release at indicated time points. Ratios of P∼Kss1p to Pgk1p and Msb2p-HA to Pgk1p relative to time 0 (set to 1) are shown. (B) Same as A except cells were pre-grown and synchronized in YEPD and released into YEP-GAL medium. (C) Quantitation of relative P∼Kss1p levels under basal (pink) and induced (blue) conditions. Data are mean±s.e.m. of three independent trials. For induced, a biological replicate from Prabhakar et al. (2020) was used for analysis. On the *x*-axis, different phases of the cell cycle were determined by time points corresponding to Clb2p levels after the release. For basal conditions, G1 (t=0), t=0; G1, t=20; G1/S, t=40; S/G2, t=60; G2/M, t=80; M, t=100; G1, t=120 min. For induced conditions, G1 (t=0), t=0; G1, t=100; G1/S, t=160; S/G2, t=200; G2/M, t=240 min. One-way ANOVA with Tukey's test was used for statistical analysis. **P*<0.05. (D) IBs of wild type (PC999) and *swi4*Δ (PC3428) in YEPD. Ratios of P∼Kss1p to Pgk1p and Msb2p-HA to Pgk1p relative to wild type (set to 1) are shown. Blot quantitation represents an average of two independent replicates. (E) Left, plate washing assay (PWA) of wild type (PC999), *swi4*Δ (PC3428) and *ste11*Δ (PC611). Middle, wild type (PC6810), *swi4*Δ (PC7626) and *ste11*Δ (PC2061) were grown on YEPD and YEPD+1M sorbitol to evaluate the HOG pathway response. Right, DIC images of wild type (PC6810), *swi4*Δ (PC7626) and *ste11*Δ (PC2061) grown in YEPD. Scale bar: 10 µm.

2009) and/or an increased fMAPK pathway activity (Fig. 3D). Although the *swi4*Δ mutant responded to α factor, the cells did not synchronize, which prevented evaluation of P∼Kss1p levels throughout the cell cycle in this mutant. These results indicate that normal cell-cycle progression impacts fMAPK pathway activity and filamentous growth.

Activation of the fMAPK pathway induces the HOG pathway

The fMAPK pathway regulates target genes that encode proteins that bring about filamentous growth (Madhani et al., 1999; Roberts et al., 2000; Vandermeulen and Cullen, 2020). A major target of the fMAPK pathway is *FLO11*, which encodes a cell adhesion molecule (Rupp et al., 1999; Vinod et al., 2008). *FLO11* expression showed a similar periodicity as *MSB2*, which indicates that its expression is regulated throughout the cell cycle (Fig. 4A). Several targets of the fMAPK pathway encode components of the pathway, and their transcriptional induction results in positive feedback that amplifies fMAPK pathway activity (Madhani et al., 1999; Roberts et al., 2000; Cullen et al., 2004; Adhikari and Cullen, 2014). Expression of genes encoding the MAP kinase, Kss1p (Fig. 4B), and the TEA/ATS-type transcription factor, Tec1p (Fig. 4C) showed similar patterns of cell-cycle regulation as *MSB2*. The transcription factor Ste12p, which functions in the mating and fMAPK pathways (Roberts and Fink, 1994), showed a different expression pattern during α factor treatment, as its expression was induced by pheromone (Fig. S3B). Therefore, key transcriptional targets of the fMAPK pathway show cell-cycle regulated expression.

To further explore activation of the fMAPK and HOG pathways, a hyperactive version of Msb2p, Msb2p$^{\Delta 100\text{-}818}$ (referred to as Msb2p**), was examined. Msb2p** induced fMAPK pathway activity, which was dependent on the transcription factor Ste12p [Fig. 4D, P∼Kss1 (Cullen et al., 2004; Vadaie et al., 2008; Prabhakar et al., 2020)]. fMAPK pathway induction occurred in basal (YEPD) and inducing (YEP-GAL) conditions (Fig. 4D). Expression of Msb2p** from an fMAPK-independent promoter also induced the fMAPK pathway through Ste12p (Fig. 4D, P∼Kss1, GAL-*MSB2*** *ste12*Δ; Prabhakar et al., 2020). This result indicates that, in addition to *MSB2*, transcriptional induction of other pathway regulators may be required for activation of the pathway. Unexpectedly, Msb2p** also stimulated the HOG pathway in a Ste12p-dependent manner (Fig. 4D, P∼Hog1). In addition to osmotic stress, the HOG pathway can be induced by galactose (Adhikari and Cullen, 2014). Ste12p also mediated HOG pathway activation by Msb2p** in YEP-GAL medium (Fig. 4D). This result indicates that transcriptional induction from the fMAPK pathway leads to activation of the HOG activity. Although we infer that positive feedback from Ste12p drives HOG pathway activation by Msb2p**, it is possible that one or more targets of the fMAPK pathway may stimulate the HOG pathway. Ste12p-dependent induction of the fMAPK pathway was higher (20-fold in GLU and GAL) than Ste12p-dependent induction the HOG pathway (ninefold in GLU and threefold in GAL, Fig. 4D,E). The activity of the HOG pathway was 18-fold higher during osmotic stress than occurs through Msb2p** (Fig. 4E). An 18-fold increase in Hog1p pathway activity may be required to elicit an adaptive response by the HOG pathway. Thus, induction of the HOG pathway by Msb2p** and Ste12p might modulate the fMAPK pathway more than the HOG pathway. Given that the HOG pathway functions antagonistically to the fMAPK pathway (Davenport et al., 1999; Adhikari and Cullen, 2014), these results describe a new type of cross-pathway regulation, where activation of one pathway (fMAPK) induces another pathway (HOG) to regulate its activity (Fig. 4F).

Sho1p levels and localization change throughout the cell cycle

To regulate the fMAPK pathway, Msb2p interacts with the tetraspan protein Sho1p (O'Rourke and Herskowitz, 1998; Cullen et al., 2004), which is a shared component between the fMAPK and HOG pathways. The level of the Sho1p protein was examined throughout the cell cycle. The level of Sho1p-GFP rose prior to accumulation in Clb2p-Myc (Fig. 5A) and dropped when P∼Kss1p increased. The drop in Sho1p-GFP during fMAPK pathway induction might be due to the turnover of active Sho1p. This possibility is based on the fact that a hyperactive version of Sho1p, Sho1p^{P120L}, shows elevated turnover compared with wild type (Adhikari et al., 2015a). The level of Sho1p-GFP also increased after 30 min of α factor treatment (Fig. 5A, Sho1-GFP), which might occur because Sho1p has a function in mating (Nelson et al., 2004). The level of *SHO1* mRNA showed cell-cycle periodicity and resembled the expression pattern of *MSB2* (Fig. 5B, orange line). Therefore, expression of genes encoding both sensors for the fMAPK pathway, *MSB2* and *SHO1*, show cell-cycle regulated gene expression.

Although Msb2p and Sho1p form a complex in the plasma membrane (Tatebayashi et al., 2015; Yamamoto et al., 2016), they have different patterns of localization and turnover (Adhikari et al., 2015a). Processed Msb2p is turned over by the E3 ubiquitin ligase Rsp5p and is turned over in the lysosome/vacuole (Adhikari et al., 2015a,b; Prabhakar et al., 2019), whereas Sho1p primarily localizes to the growth tip in developing buds and the mother-bud neck in large buds (Raitt et al., 2000; Reiser et al., 2003; Pitoniak et al., 2009). To better understand the contribution of Msb2p and Sho1p in the cell-cycle regulation of the fMAPK pathway, time-lapse fluorescence microscopy was performed. Msb2p-GFP and Sho1p-GFP fusion proteins were examined in cells expressing the septin Cdc3p-mCherry, which shows a distinct pattern of localization throughout the cell cycle (Kim et al., 1991; Lippincott et al., 2001). Owing to its high turnover rate (Adhikari et al., 2015a,b), Msb2p-GFP showed a predominantly vacuolar localization pattern, which may result from the stability of the GFP protein in vacuoles (Movie 1). By comparison, Sho1p-GFP localized to presumptive bud sites, the tip of developing buds and the mother-bud neck as

Journal of Cell Science (2021) 134, jcs258341. doi:10.1242/jcs.258341

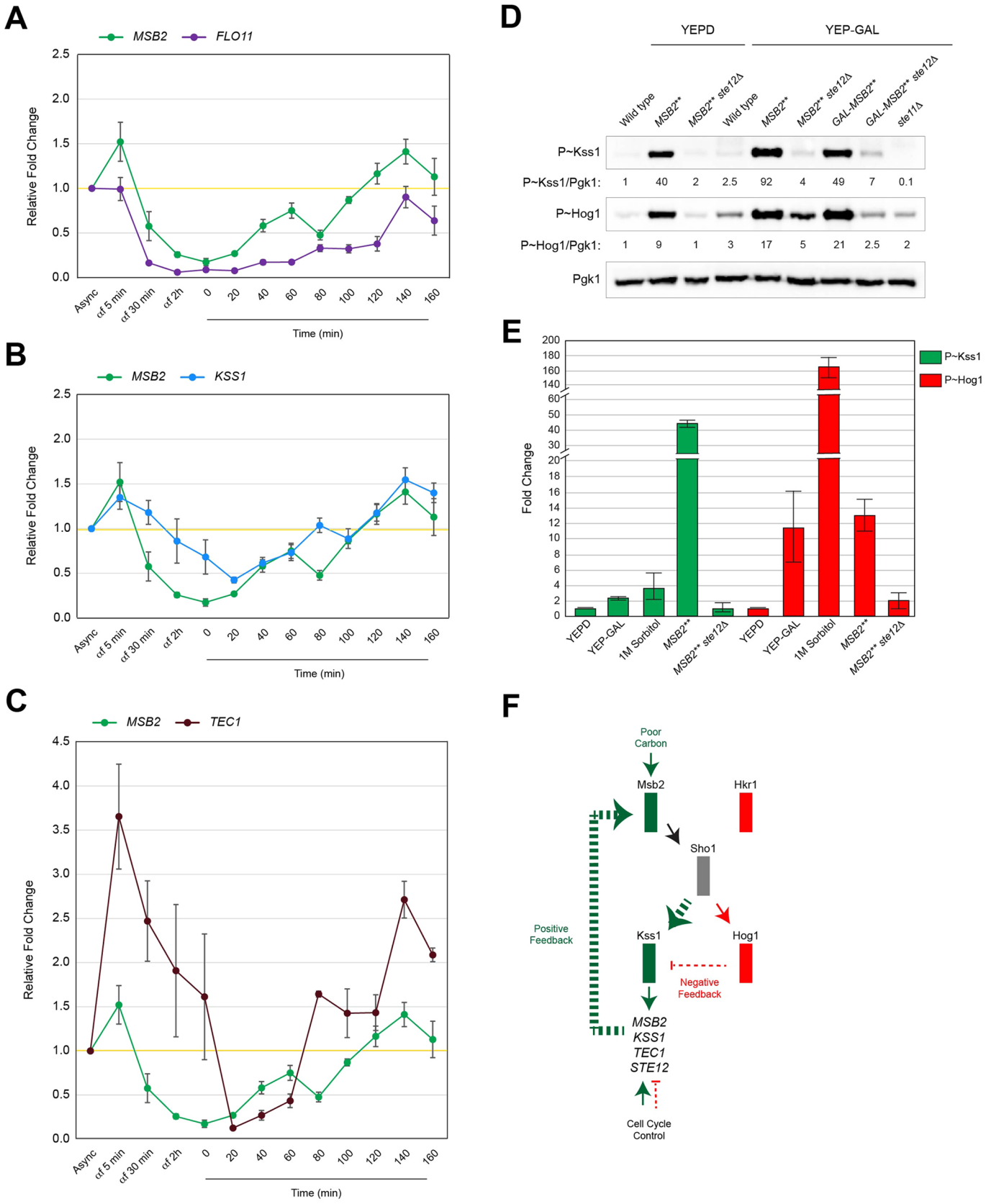

Fig. 4. See next page for legend.

Fig. 4. Expression profile of fMAPK components throughout the cell cycle and role of cross-pathway regulation in regulating fMAPK and HOG pathway activities. (A) Fold changes in the mRNA levels of *MSB2* (green) and *FLO11* (purple) at indicated time points in synchronized cells relative to the asynchronous culture (Async). *MSB2* values were taken from Fig. 2D. See Fig. 2D for details. The fluctuations in *FLO11* mRNA levels were statistically significant at some time points (P<0.01). Specifically, αf=30 min, αf=2 h, t=0 min-120 min were different from other time points. (B) As in A, for levels of *MSB2* (green) and *KSS1* (blue). The fluctuations in *KSS1* mRNA levels at t=20 min and t=140 min were different from other time points. (C) As in A, for levels of *MSB2* (green) and *TEC1* (brown). The fluctuations in *TEC1* mRNA levels at αf=5 min and at t=140 min were statistically different from other time points. (D) Immunoblots (IBs) of wild type (PC538), *MSB2*** (PC1516) and *MSB2*** *ste12*Δ (PC1811) grown in YEPD and YEP-GAL; and *GAL-MSB2*** (PC1806), *GAL-MSB2*** *ste12*Δ (PC1837) and *ste11*Δ (PC611) grown in YEPG-GAL. Ratios of P∼Kss1p to Pgk1p and P∼Hog1p to Pgk1p relative to wild type in YEPD (set to 1) are shown. (E) Comparison of P∼Kss1p and P∼Hog1p levels in the indicated strains under basal and pathway-inducing conditions for the fMAPK and HOG pathways. The histogram represents the ratio of P∼Kss1p to Pgk1p and P∼Hog1p to Pgk1p relative to wild-type (set to 1). Data are mean ±s.e.m. of three independent trials. Green, P∼Kss1p; red, P∼Hog1p. (F) One model showing role of poor carbon source, cell cycle, transcriptional induction of pathway components and the HOG pathway in regulating the activity of the fMAPK pathway. Arrows and proteins shown in green refer to induction; lines, arrow and proteins shown in red refer to inhibition; the cell cycle has inducing and inhibiting effects depending on the stage. Sho1, shared protein. Dashed green arrows indicate a preferential stimulation of the fMAPK pathway through a transcriptional induction loop that involves Msb2p.

cells progressed through the cell cycle (Movies 2 and 3). The same pattern was seen under inducing conditions (GAL media), except that Sho1p-GFP was localized to the distal pole for an extended period (Movie 4). Because cells grown under inducing conditions bud distally, the localization of Sho1p-GFP to the mother-bud neck was readily detected and occurred when the septin ring split into a double ring prior to cytokinesis [Movie 4 (Kim et al., 1991; Lippincott et al., 2001; Bi and Park, 2012)].

Based on P∼Kss1p analysis, Sho1p-GFP can transduce signals to the fMAPK pathway from different sites on the plasma membrane. Moreover, in synchronized cells, the increase in P∼Kss1p levels at M/G1 (Fig. 5A, P∼Kss1, 100 min) corresponded to Sho1p-GFP localization at the mother-bud neck (Fig. S4A, 100 min, 45%±2.5 in synchronous cells compared to 11% in asynchronous cells). A challenge connecting Sho1p localization to fMAPK pathway activity is that protein localization is evaluated by microscopy, whereas MAPK activity is evaluated by immunoblot analysis. In mammalian cells, the localization of P∼ERK has been evaluated by immunofluorescence (IF), which has revealed insights into the spatial and temporal nature of MAPK pathway signaling (Shapiro et al., 1998; Ingram et al., 2000; Molgaard et al., 2016). One problem in detecting P∼Kss1p by IF is interference from other P∼ERK type MAPKs. Antibodies that detect P∼Kss1p also recognize P∼Slt2p, which regulates the cell wall integrity pathway (Lee et al., 1993). To circumvent this problem, the *SLT2* gene was disrupted. In the *slt2*Δ mutant, P∼Kss1p was the main band detected using a phospho-MAPK specific antibody that preferentially detects P∼Kss1p over P∼Fus3p (Fig. 5C, *slt2*Δ). Accordingly, the level of P∼Kss1p was higher in cells carrying Msb2p** and reduced in cells lacking the MAPKKK Ste11p (Fig. 5C). An Alexa 647 fluorophore-conjugated secondary antibody showed the same pattern by immunoblot (Fig. 5C) and detected P∼Kss1p by IF (Fig. 5D). Cells grown in YEP-GAL media showed a higher P∼Kss1p signal than cells grown in YEPD medium (Fig. 5D). Therefore, IF can be used to evaluate P∼Kss1p activity.

Like many MAPKs, mammalian ERK1/2 proteins (also known as MAPK3 and MAPK1, respectively) enter the nucleus upon activation (Chen et al., 1992; Lenormand et al., 1993; Pouysségur et al., 2002; Zehorai et al., 2010). By comparison, Kss1p has a unique regulatory mechanism. Unphosphorylated Kss1p is present in the nucleus in an inhibitory complex with Ste12p, Tec1p and Dig1p (Bardwell et al., 1996; Cook et al., 1997; Bardwell et al., 1998). Upon phosphorylation by Ste7p, active Kss1p phosphorylates Ste12p, Tec1p and Dig1p, and exits the nucleus (Ma et al., 1995; Bardwell et al., 1998; Pelet, 2017). Consistent with this mechanism, P∼Kss1p was localized in the cytoplasm in a non-uniform pattern (Fig. 5D). We next evaluated the level of P∼Kss1p throughout the cell cycle. P∼Kss1p levels were higher in M/G1, based on the signal intensity of mitotic and post-mitotic cells where the nucleus was visible in mother and daughter cells (Fig. S4B, normalized fluorescence). Total Kss1p levels in synchronized cells do not fluctuate as cells progress through the cell cycle (Prabhakar et al., 2020). In cells in which Sho1p-GFP was localized to the mother-bud neck, P∼Kss1p levels were higher than in cells where Sho1p-GFP was localized in buds (Fig. 5E,F). The 1.8-fold increase reported by single-cell immunofluorescence matched the 1.9-fold increase seen by IB analysis (average values of Figs 1,2,3 and 5). Therefore, Sho1p is localized to the mother-bud neck when cells show elevated fMAPK pathway activity in M/G1.

Cytokinesis regulatory protein Hof1p regulates the fMAPK pathway

Given that the fMAPK pathway can be induced by proteins that localize to the mother-bud neck, we explored the role of other proteins at the mother-bud neck in regulating fMAPK pathway signaling. Septins are hetero-oligomers that form a cytoskeletal ring at the mother-bud neck, and control bud emergence, cytokinesis and mother-daughter asymmetry (Hall et al., 2008; McMurray and Thorner, 2009; Bi and Park, 2012). Although septins are essential, temperature-sensitive alleles can allow evaluation of septin function. The *cdc12-6* mutant shows normal growth at 25°C and is inviable at 37°C. At 30°C, the *cdc12-6* mutant exhibits cytokinesis defects and shows defects in fMAPK pathway activity by immunoblot (IB) analysis (Fig. 6A). The *cdc12-6* mutant also showed reduced *FUS1-lacZ* (Fig. S5A) and *FUS1-HIS3* reporter activity (Fig. S5B), which in strains lacking an intact mating pathway (*ste4*Δ) requires the fMAPK pathway (Cullen et al., 2004). Sho1p-GFP was mis-localized in the *cdc12-6* mutant at 30°C (Fig. 6B, arrows). The *cdc12-6* mutant also showed a defect in fMAPK pathway activity at 25°C (Fig. S5A and B) due to a bud-site-selection defect (Basu et al., 2016). Therefore, proper septin function is required for fMAPK pathway activity and Sho1p localization.

At the mother-bud neck, Sho1p interacts with proteins that regulate cytokinesis (Labedzka et al., 2012). One such protein is Hof1p, an Fes/CIP4 homology-Bin/Amphiphysin/Rvs (F-BAR) type protein that localizes to the mother-bud neck prior to cytokinesis and moves to the actomyosin ring during cytokinesis to regulate cell separation (Vallen et al., 2000; Meitinger et al., 2011; Oh et al., 2013). *HOF1* and other genes that regulate cytokinesis were disrupted in the filamentous (Σ1278b) background. The *hof1*Δ mutant, but not the *cyk3*Δ, *bni5*Δ or *shs1*Δ mutants, showed a defect in fMAPK pathway activity based on P∼Kss1p levels (Fig. 6C) and *FUS1-HIS3* reporter activity (Fig. 6D, Fig. S5C). The *hof1*Δ mutant was also defective for invasive growth by the plate-washing assay (Fig. 6D) and for the formation of filamentous cells (Fig. 6E) by the single-cell invasive growth assay (Cullen and Sprague, 2000). Together, each of these tests indicate that Hof1p regulates the fMAPK pathway.

Journal of Cell Science (2021) 134, jcs258341. doi:10.1242/jcs.258341

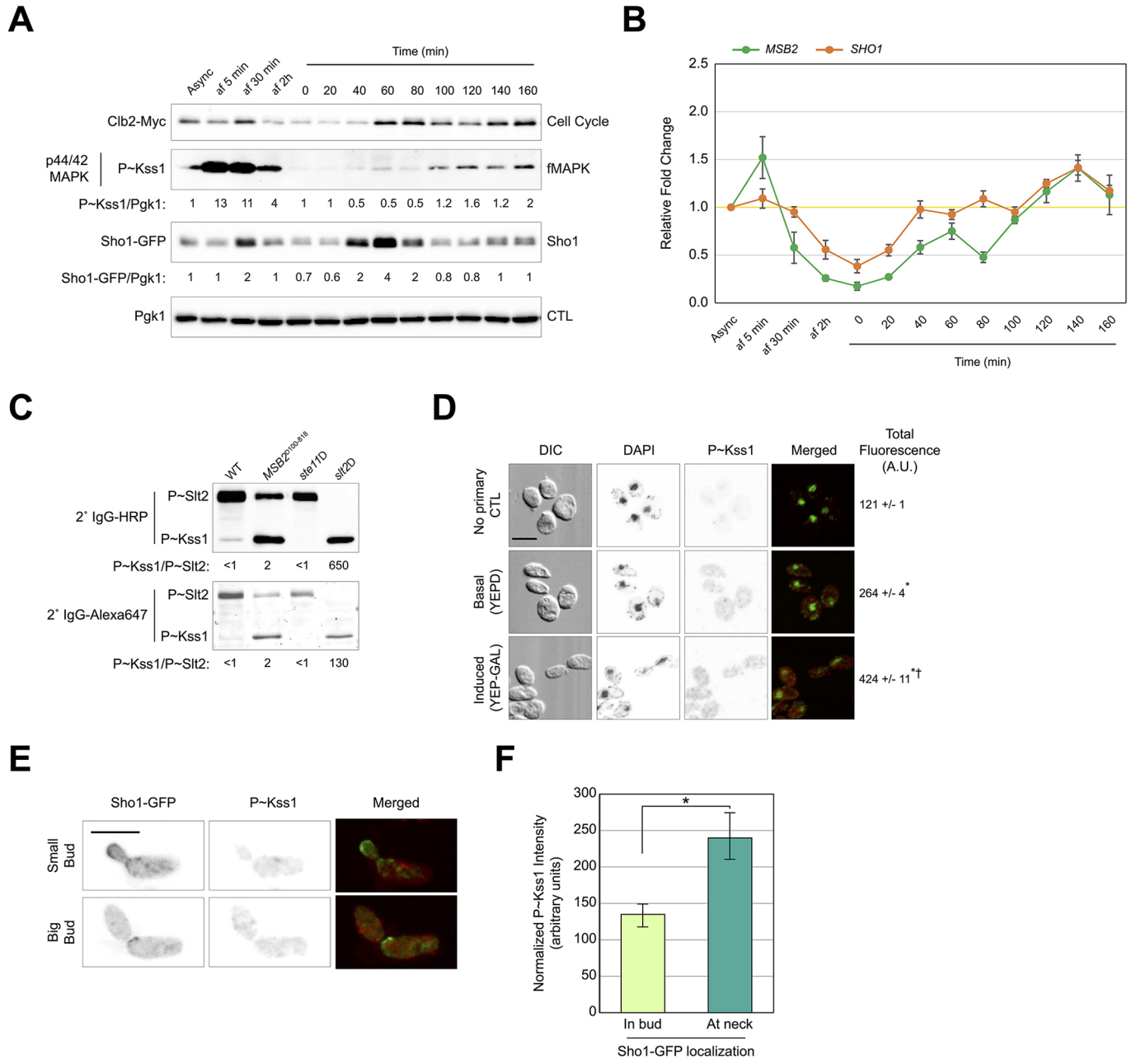

Fig. 5. Levels, expression and localization of Sho1p throughout the cell cycle. (A) Immunoblots (IBs) of wild type containing Sho1p-GFP (PC7495+p*STE4*+p*SHO1-GFP::NAT*) synchronized in G1 and released into YEPD. Samples were harvested and probed as in Fig. 1B. Ratios of P~Kss1p to Pgk1p and Sho1p-GFP to Pgk1p relative to time 0 (set to 1) are shown. (B) Fold change in the mRNA levels of *MSB2* (green) and *SHO1* (orange) at indicated time points in synchronized cells relative to the asynchronous culture (Async). See Fig. 2D for details. *MSB2* values were taken from Fig. 2D. Based on ANOVA with Dunnett's statistical test, the fluctuations in *SHO1* mRNA levels at αf=2h, t=0 min, t=20 min and t=140 min were significantly different from other time points. (C) IBs of wild type (PC538), *MSB2*** (PC1516), *ste11*Δ (PC611) and *slt2*Δ (PC3394) using HRP-conjugated or Alexa 647-conjugated secondary antibody. Ratios of P~Kss1p to P~Slt2p levels. (D) Indirect immunofluorescence of the *slt2*Δ mutant. Mid-log cells grown in YEPD were stained with or without anti-p44/42 (ERK1/2) rabbit primary antibody followed by co-staining with anti-rabbit goat Alexa 647 secondary antibody and DAPI. Mid-log cells grown in YEP-GAL were also stained with primary antibody, secondary antibody and DAPI. Numbers refer to total fluorescence intensity calculated for each cell after subtracting background intensity from the mean fluorescence intensity of each cell. Data are mean±s.e.m. from 50 cells. A two-tailed *t*-test was used for statistical analysis. *P<0.05, intensity values in panels where primary antibody was added (basal and induced) were significantly different from the no primary control; †P<0.05, intensity values in the induced condition were significantly different from other panels. Scale bar: 5 µm. (E) Indirect immunofluorescence of *slt2*Δ cells containing Sho1p-GFP (PC3394+p*SHO1-GFP::NAT*). Representative cells where Sho1p-GFP is present in the bud cortex (small bud) or at the mother-bud neck (large bud) are shown. Cells were grown to mid-log in YEP-GAL. Scale bar: 5 µm. (F) Quantitation of normalized pixel intensity of P~Kss1p from cells in E. Data are mean±s.e.m. for 15 cells. A two-tailed *t*-test was used for statistical analysis. Intensity values in large buds with Sho1p-GFP at neck were different from those in small buds with Sho1p-GFP in bud cortex (*P<0.05). A.U., arbitrary units.

Journal of Cell Science (2021) 134, jcs258341. doi:10.1242/jcs.258341

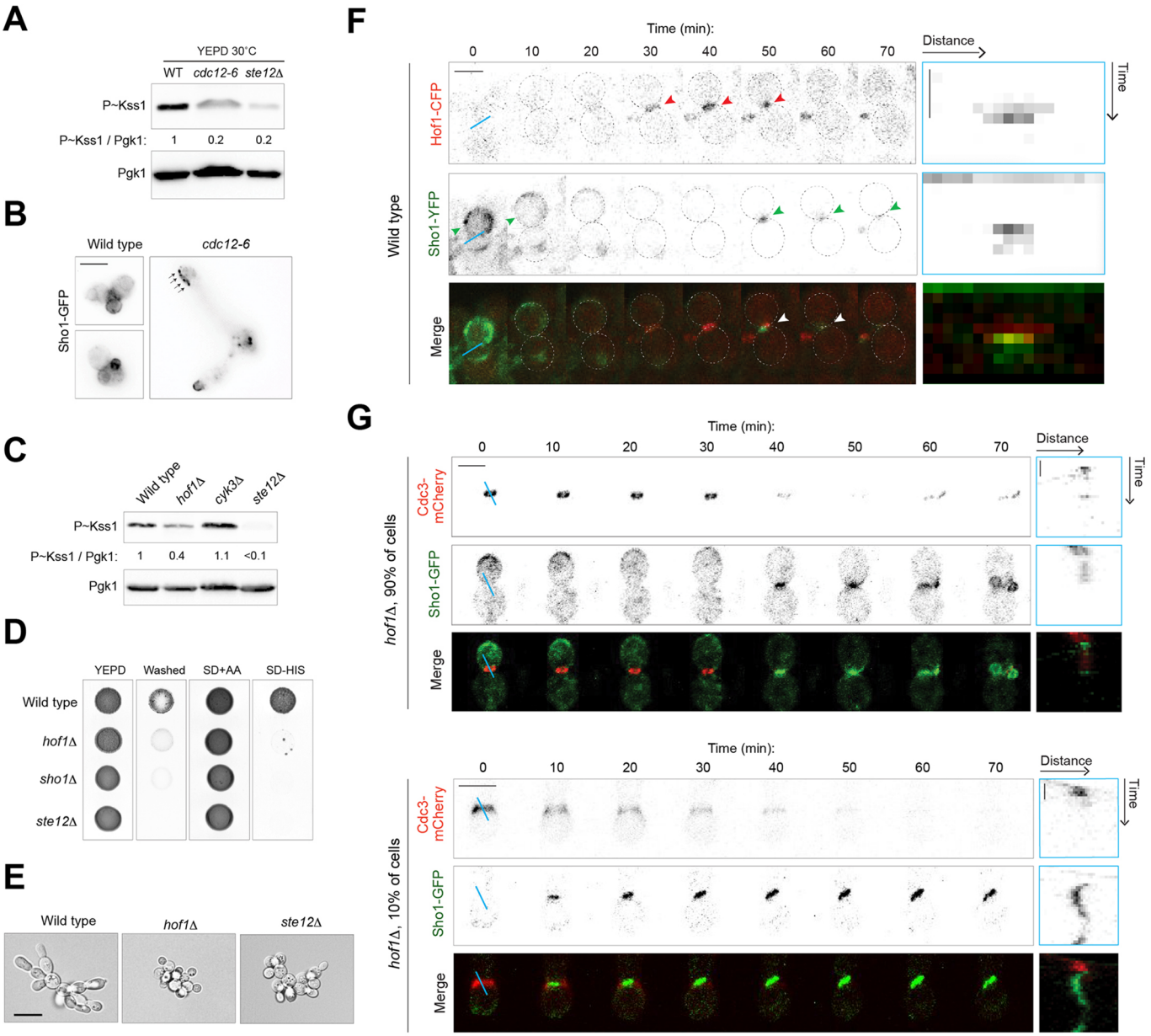

Fig. 6. Role of septins and Hof1p in regulating the fMAPK pathway. (A) Immunoblots (IBs) of wild type (PC538), *cdc12-6* (PC2710) and *ste12*Δ (PC539) grown for 6 h in YEPD medium. Ratios of P~Kss1p to Pgk1p relative to wild type (set to 1) are shown. (B) Wild type and the *cdc12-6* mutant carrying pSho1p-GFP were grown to mid-log stage in YEPD medium at 30°C. Representative cells are shown. Scale bar: 5 µm. (C) IBs of wild type (PC538), *hof1*Δ (PC2371), *cyk3*Δ (PC6472) and *ste12*Δ (PC539) strains grown to mid-log phase in YEPD medium. See A for details. (D) Plate washing assay (PWA) and *FUS1-HIS3* growth reporter activity. (E) Single-cell assay for the indicated strains. Scale bar: 10 µm. (F) Localization of Hof1p-CFP and Sho1p-YFP (PC2377) over time. Top, red arrows indicate Hof1p-CFP and green arrows indicate Sho1p-YFP. A merged image is shown, see Movie 5. Right, kymograph analysis of the mother-bud neck, denoted by the blue line in the top panel. Black and white images are false colored to improve visualization. Kymograph scale is 50 min. (G) Sho1p-GFP and Cdc3p-mCherry localization in the *hof1*Δ mutant (PC7563+p*SHO1-GFP*). Top, representative localization patterns are shown (90% of cells show normal localization Movie 6, 10% of cells show irregular localization Movie 7). Right, kymograph analysis of the mother-bud neck, indicated by the blue line in the top panel. Kymograph scale is 50 min. Scale bars in F,G: ∼5 µm.

Because the cytokinesis regulator Hof1p interacts with Sho1p, which also localizes to the mother-bud neck prior to cytokinesis (Movie 4), we explored whether the proteins co-localize by time-lapse microscopy. Sho1p-YFP and Hof1p-CFP localized to the mother-bud neck in temporally distinct patterns (Fig. 6F, kymograph, Movie 5). Prior to cytokinesis, Hof1p-CFP localized to the neck (30 min, red arrow). Sho1p-YFP localized to the neck after the arrival of Hof1p (50 min, green arrow) and remained there after Hof1p was no longer detected at that site. Based on this pattern, we tested whether Hof1p impacted Sho1p localization to the mother-bud neck. By analyzing the localization of Sho1p-GFP in cells lacking Hof1p, we found that most cells showed a normal pattern of Sho1p-GFP localization (Fig. 6G, Movie 6). However, Sho1p was mis-localized in 10% of *hof1*Δ cells, which showed a delay in cytokinesis. In these cells, Sho1p-GFP remained at the bud neck for extended periods (Fig. 6G, kymographs; 240 min, Movie 7). Thus, although Hof1p may play a role in Sho1p localization, this may not fully account for the MAPK signaling

Journal of Cell Science (2021) 134, jcs258341. doi:10.1242/jcs.258341

Table 1. Patterns of bud-site selection for mutants lacking proteins that regulate cytokinesis

Strain	Proximal	Distal	Equatorial	fMAPK‡
Wild type	88	10	2	1.00
*hof1*Δ	71	24	5	0.11
*cyk3*Δ	78	15	7	1.35
*bni5*Δ	59	32	9	1.09
*shs1*Δ	55	32	13	1.02
*bud3*Δ	3	80	17	<0.1§

Budding pattern (proximal, distal or equatorial) was determined as described in the Materials and Methods; values refer to numbers of cells that showed the indicated bud-site selection pattern.

‡fMAPK pathway activity was determined by quantitation of the activity of the *FUS1-HIS3* reporter (see Fig. S6B). Wild-type values were set to 1. Other values were adjusted accordingly.

§Based on analysis of previously reported data (Basu et al., 2016).

defect of the *hof1*Δ mutant. *SHO1* also showed genetic interactions with *HOF1*. Specifically, overexpression of *SHO1*, which induces hyperpolarized growth (Vadaie et al., 2008; Pitoniak et al., 2015), exacerbated the growth defect of the *hof1*Δ mutant (Fig. S5D). Bud-site-selection proteins that control axial budding also localize to the mother-bud neck (Chant et al., 1995; Sanders and Herskowitz, 1996) and regulate the fMAPK pathway (Basu et al., 2016). The *hof1*Δ mutant had a defect in bud-site selection (Table 1, Fig. S5E), which was less severe than that seen in axial budding mutants (Table 1, *bud3*Δ). The bud-site-selection defect of the *hof1*Δ mutant may not account for its signaling defect in the fMAPK pathway, because cytokinesis regulators that had more severe bud-site-selection defects did not impact fMAPK pathway activity (Table 1, Fig. S5E). Therefore, Hof1p, which interacts with Sho1p, localizes to the mother-bud neck and regulates cytokinesis, also regulates the fMAPK pathway.

DISCUSSION

Cell-cycle regulation of MAPK pathway activity

MAPK pathways commonly alter cell-cycle progression. In yeast, MAPK pathways alter the progression of the cell cycle during mating (Strickfaden et al., 2007), during filamentous growth (Madhani et al., 1999) and in response to osmotic stress (Waltermann et al., 2010; Radmaneshfar et al., 2013). Mammalian ERKs induce entry into the cell cycle from a G_0 state (Seger et al., 1994) and regulate G1/S (Aktas et al., 1997; Leone et al., 1997) and G2/M (Wright et al., 1999; Dangi et al., 2006) transitions, including the regulation of mitosis (Shapiro et al., 1998). By comparison, how the activity of MAPK pathways are themselves cell-cycle regulated is less well understood. Here, we show that the activity of the fMAPK pathway, which controls a cell differentiation response in yeast, is cell-cycle regulated (Fig. S6). fMAPK pathway activity is low in G1, S and G2, and high in M/G1. By comparison, the HOG pathway, which shares some components with the fMAPK pathway, can be activated by osmotic stress at any point in the cell cycle (here and Nagiec and Dohlman, 2012). The fact that the HOG pathway can be induced independently of the cell cycle may not be surprising as cells can encounter osmotic stress at any point in the growth cycle.

The activity of the fMAPK pathway may be tied to the cell cycle in several ways. One way is at the level of expression of the gene encoding the mucin Msb2p. We show here that the expression of *MSB2* shows cell-cycle periodicity. *MSB2* expression is controlled by multiple signaling pathways (Chavel et al., 2010), and we also show that the G1/S transcription factor Swi4p regulates the fMAPK pathway and filamentous growth. Swi4p may regulate the fMAPK pathway by regulating *MSB2* expression. The *MSB2* promoter contains the regulatory element CACGAAA (Breeden and Nasmyth, 1987) 466 bp upstream of the start site, which can be recognized by Swi4p (Iyer et al., 2001; MacIsaac et al., 2006). This regulatory element is near two Ste12p-binding sites [(A)TGAAACA] at 474–481 and 522–530 bp (Cullen et al., 2004). Although Swi4p and Swi6p are positive regulators of G1/S transcription, how Swi4p negatively regulates fMAPK pathway activity remains unclear. Interestingly, growth of cells in galactose partially overrides the cell-cycle regulation of the fMAPK pathway. This might result from induction of *MSB2* expression by a protein or pathway that is activated under nutrient-limiting conditions that induce filamentous growth. Elevated processing of the Msb2p protein, which is required for fMAPK pathway activity and occurs at elevated levels in galactose (Vadaie et al., 2008), might also be subject to cell-cycle control.

Another way the activity of the fMAPK pathway may be tied to the cell cycle is through the adaptor protein Sho1p. We show that, like *MSB2*, expression of the *SHO1* gene shows cell-cycle periodicity. Several transcription factors that regulate cell-cycle progression bind to the *SHO1* promoter, including Fhk1p (Ostrow et al., 2014) and Mbp1p (MacIsaac et al., 2006). Whether these proteins impart cell-cycle regulation to *SHO1* remains to be determined. It has previously been shown that *TEC1* expression is induced at the M/G1 boundary by Swi5p, a transcription factor that functions at the G1 phase of the cell cycle (Cho et al., 1998; Spellman et al., 1998; Wittenberg and Reed, 2005). Therefore, cell-cycle regulation of the fMAPK pathway may occur by regulating the expression of genes encoding multiple pathway components, by the action of several cell-cycle regulatory transcription factors.

Coupling the activity of the fMAPK pathway to the cell cycle may allow the pathway to carry out cell-cycle-dependent functions. For example, we have recently shown that, under filamentous conditions, the fMAPK pathway regulates the intrinsic polarity pathway of the cell, which occurs in G1, to promote bud emergence (Prabhakar et al., 2020). The fMAPK pathway also regulates cell differentiation to filamentous growth. One MAPK-dependent change that occurs during filamentous growth is increased cell adhesion mediated by the major cell-adhesion molecule Flo11p. We show here that the expression of the *FLO11* gene is regulated throughout the cell cycle. Flo11p is required to control adhesion functions under a variety of conditions, including nutrient-replete conditions (Pitoniak et al., 2009; Basu et al., 2016) and may have biological effects on mating (Guo et al., 2000). Moreover, the periodic expression of *FLO11* throughout the cell cycle may impact its role in adhesion, which occurs at the mother-bud neck, presumably after cytokinesis has occurred. Another target of the fMAPK pathway, *BUD8* (Adhikari and Cullen, 2014), which marks the distal pole and is required for distal budding during filamentous growth (Taheri et al., 2000; Harkins et al., 2001; Cullen and Sprague, 2002), is tightly regulated throughout the cell cycle to ensure proper cell polarity (Schenkman et al., 2002). During filamentous growth, the fMAPK pathway induces a delay in the cell cycle by stimulating expression of the gene encoding the G1 cyclin Cln1p (Loeb et al., 1999; Madhani et al., 1999). Therefore, the cell-cycle regulation of a MAPK pathway may impart cell-cycle regulation to target genes to ensure that aspects of the morphogenetic response are tightly coordinated.

Interestingly, human MEK and ERK kinases are also activated during mitosis in somatic cells to regulate the spindle assembly checkpoint (Shapiro et al., 1998; Horne and Guadagno, 2003; Rosner, 2007; Cao et al., 2010), proper entry into anaphase (Shapiro

et al., 1998; Roberts et al., 2002) and fragmentation of Golgi cisternae (Acharya et al., 1998; Cha and Shapiro, 2001; Shaul and Seger, 2006). Therefore, MAPK pathways may have a general role in regulating events that occur throughout the cell cycle, necessitating that the pathways themselves exhibit cell-cycle-dependent activity (Pagès et al., 1993; Mansour et al., 1994; Wright et al., 1999; Katz et al., 2007).

Cross-pathway regulation between MAPK pathways

Functional interactions between signaling pathways can modulate pathway outputs. Here, we show that activation of the fMAPK pathway induces HOG pathway activity, presumably to modulate fMAPK pathway activity. Cross-pathway feedback occurs due to pathway hyperactivation and may occur under normal circumstances, because both the fMAPK pathway and the HOG pathway are induced by growth of cells in non-preferred carbon sources (Adhikari and Cullen, 2014). Modulation of fMAPK pathway activity is important for generating an appropriate response, as elevated fMAPK pathway activity creates morphogenetic problems (Prabhakar et al., 2020).

The mother-bud neck: a hub for MAPK pathway signaling?

Several proteins that function at the mother-bud neck regulate the fMAPK pathway. These proteins include axial markers that control bud-site selection proteins (Basu et al., 2016), cytokinesis remnant proteins (Prabhakar et al., 2020), the septins themselves (this study) and the cytokinesis regulator Hof1p (this study). Hof1p may regulate the fMAPK pathway through interaction with Sho1p (Labedzka et al., 2012), as well as through its role in regulating septin reorganization during cytokinesis (Meitinger et al., 2013). The Hof1p-interacting protein Cyk3p (Labedzka et al., 2012) does not impact the activity of the fMAPK pathway. Hof1p and Cyk3p may recruit non-overlapping proteins to the mother-bud neck that impact Sho1p function or activity. Future work may elucidate how functionally distinct proteins at the mother bud neck contribute to the regulation of a MAPK pathway.

MATERIALS AND METHODS

Strains and plasmids

Yeast strains are described in Table S1. Gene disruptions were made with antibiotic resistance markers *KanMX6* (Longtine et al., 1998), *HYG* and *NAT* (Goldstein and McCusker, 1999) using PCR-based methods. Pop-in pop-out strategy was used to make internal epitope fusions (Schneider et al., 1995). Some strains were made *ura3*$^{-}$ by selection on 5-fluoroorotic acid (5-FOA). Gene disruptions were confirmed by PCR-based Southern analysis and also by phenotype when applicable. The *swi6*Δ mutant had a severe growth defect, which prevented evaluation of fMAPK and HOG pathway activities.

Most of the plasmids used in this study belong to the pRS series of plasmids (pRS315 and pRS316) (Sikorski and Hieter, 1989). p*GFP-MSB2* (Adhikari et al., 2015b), pRS316-*SHO1-GFP* (Marles et al., 2004), p*SHO1*^{P120L} (Vadaie et al., 2008), p*SHO1-GFP::NAT* (Prabhakar et al., 2020), pMyr-*SHO1* and pMyrAS-*SHO1* (Raitt et al., 2000), YCp50-*STE11-4* (Stevenson et al., 1992) and p*STE4* (Stevenson et al., 1992) have been described previously.

Microbial techniques

Standard methods were followed during yeast and bacterial strain manipulations (Sambrook et al., 1989; Rose et al., 1990). Budding pattern was determined as described previously (Cullen and Sprague, 2002). The activity of the *FUS1-HIS3* (McCaffrey et al., 1987) growth reporter in cells lacking an intact mating pathway (*ste4*Δ) is dependent on components of the fMAPK pathway (Cullen et al., 2004) and was determined by growth of cells on media lacking histidine and supplemented with ATA (3-amino-1,2,4-triazole) for 3 days. β-Galactosidase assays to assess the activity of the *FUS1-lacZ* reporter were performed as described previously (Cullen et al., 2000). The single-cell invasive growth assay (Cullen and Sprague, 2000) and the plate-washing assay (Roberts and Fink, 1994) have been previously described. For the single cell assay, cells were grown for 12 h at 30°C on synthetic complete media lacking glucose.

Immunoblot analysis

Immunoblot (IB) analysis to detect phosphorylated MAPKs has been described previously (Sabbagh et al., 2001; Lee and Dohlman, 2008; Basu et al., 2016; Prabhakar et al., 2020). Proteins were precipitated from cell pellets stored at −80°C by trichloroacetic acid (TCA) and analyzed on 10% sodium dodecyl sulfate polyacrylamide gel electrophoresis (SDS-PAGE). Proteins were transferred to nitrocellulose membranes (Amersham Protran Premium 0.45 µm NC, GE Healthcare Life Sciences, 10600003). For Msb2p-HA and Hkr1p-HA blots, 6% acrylamide gel was used.

ERK-type MAP kinases (P∼Kss1p, P∼Fus3p and P∼Slt2p) were detected using α-p44/42 antibodies (Cell Signaling Technology, 4370 and 9101) at a 1:5000 dilution. 9101 produced a stronger signal for P∼Kss1p than for P∼Fus3p, while 4370 detected both proteins with similar strength. α-p38-type antibody at 1:5000 dilution (Cell Signaling Technology, MA 9211) was used to detect P∼Hog1p. α-HA antibody at a 1:5000 dilution (Roche Diagnostics, 12CA5) was used to detect Clb2p-HA, Msb2p-HA and Hkr1p-HA. Clb2p-Myc was detected using α-c-Myc antibody at 1:5000 dilution (Santa Cruz Biotechnology, 9E10) and Sho1p-GFP was detected using α-GFP antibody at 1:5000 dilution (Roche Diagnostics, clones 7.1 and 13.1, 11814460001). α-Pgk1 antibody was used at a 1:5000 dilution for total protein levels (Novex, 459250). For secondary antibodies, goat α-rabbit secondary IgG-HRP antibody was used at a 1:10,000 dilution (Jackson ImmunoResearch Laboratories, 111-035-144). Goat α-mouse secondary IgG-HRP antibody was used at a 1:5000 dilution (Bio-Rad Laboratories, 170-6516). Phospho-MAPK antibodies were incubated in 1× TBST [10 mM TRIS-HCl (pH 8), 150 mM NaCl, 0.05% Tween 20] with 5% BSA. For all other antibodies, 1× TBST with 5% non-fat dried milk was used. Primary incubations were carried out for 16 h at 4°C. Secondary incubations were carried out for 1 h at 25°C.

Cell synchronization and cell-cycle experiments

Cell synchronization by elutriation (Rosebrock, 2017) was not feasible for cells of the ∑1278b background because cells fail to separate, even those lacking the adhesion molecule Flo11p (Vandermeulen and Cullen, 2020). Cell synchronization experiments were performed as previously described (Breeden, 1997; Prabhakar et al., 2020). Overnight cultures were resuspended in fresh media and grown to an optical density (OD) A_{600} of 0.2 at 30°C. Strains that required synthetic media (SD-URA) to maintain plasmid selection were harvested and resuspended in an equal volume of YEPD and incubated for 1 h at 30°C prior to α factor treatment. A 10 ml aliquot was harvested for asynchronous culture. To arrest cells in G1, α factor was added to a final concentration of 5 µg/ml and the culture was incubated for 2 h at 30°C. 10 ml aliquots were harvested at 5 min, 30 min and 2 h during α factor treatment. To arrest cells in S phase, hydroxyurea (HU) (MilliporeSigma, H8627) was added to a final concentration of 400 mM and incubated for 4 h. Arrested cells were washed twice with water (pre-warmed at 30°C) and resuspended in fresh YEPD or YEP-GAL media (pre-warmed at 30°C) to release cells into the cell cycle. 10 ml aliquots were harvested every 10 or 20 min and stored at −80°C.

DIC and fluorescence microscopy

Differential-interference-contrast (DIC) and fluorescence microscopy using FITC and TRITC filter sets were performed using an Axioplan 2 fluorescent microscope (Zeiss) with a Plan-Apochromat 100×/1.4 (oil) objective (N.A. 1.4) (cover slip 0.17) (Zeiss). Digital images were obtained at multiple focal planes with the Axiocam MRm camera (Zeiss) and Axiovision 4.4 software (Zeiss). Adjustments to brightness and contrast were made in Adobe Photoshop.

Time-lapse microscopy was performed on a Zeiss 710 confocal microscope equipped with a Plan-Apochromat 40×/1.4 Oil DIC M27 objective. Lasers were used as follows: for GFP, 488 nm (496nm-548 nm filter); for mCherry, 580 nm (589nm-708 nm filter); for YFP, 517 nm (532-620 filter); for CFP, 458 nm (462-532 filter). Images were captured at 10 min intervals as follows: for Sho1p-GFP time lapse, nine *z*-stacks 1 µm thick; for GAL-GFP-Msb2p time lapse, six *z*-stacks 0.6 µm thick; and for Hof1p-CFP and Sho1p-YFP co-localization, eight *z*-stacks 1.2 µm thick.

Cells for time-lapse and co-localization studies were prepared as described previously (Prabhakar et al., 2020). Cells were grown at 30˚C for 16 h in SD-URA and diluted to <0.1 O.D. 10 µl of diluted cells were placed under agarose pad (1%) prepared inside a 12 mm Nunc glass base dish (150680, Thermo Scientific). 100 µl of water was placed in the dish to prevent the agarose pad from drying and the Petri dish was incubated at 30°C for 4 h prior to imaging.

Indirect immunofluorescence

Indirect immunofluorescence was performed as previously described with the following modifications (Amberg et al., 2006; Schnell et al., 2012). Cells were grown to mid-log stage and 8% fresh paraformaldehyde (PFA) prepared in PBS (pH 7.4) was added directly to the culture (final concentration, 4%) for 10 min with shaking. Cells were harvested for 3 min at 350 ***g*** and resuspended in KM solution [40 mM KPO_4 (pH 6.5), 500 µM $MgCl_2$] containing 4% PFA for 1 h at 30°C with gentle shaking. Cells were washed twice with KM solution and once with KM solution containing 1.2 M sorbitol. After the last wash, cells were resuspended in 500 µl KM solution containing 1.2 M sorbitol and 60 µl Zymolyase (50 mg/ml 20T) for 20 min at 37°C. During Zymolyase treatment, samples were periodically examined by DIC microscopy for cells with dull gray appearance and intact morphology (Niu et al., 2011). After Zymolyase treatment, cells were washed at 300 ***g*** with KM solution containing 1.2 M sorbitol and resuspended in the same solution. Wells of Teflon-faced slides (MP Biomedicals, 096041205) were coated with 20 µl poly-L-lysine (Cultrex Poly-L-Lysine, Bio-Techne, 3438-100-01) and incubated for 10 min at 24°C in a humid chamber. All solutions were centrifuged at 16,000 ***g*** for 20 min at 4°C prior to adding to the wells. Wells were washed five times with 20 µl water and air dried. 20 µl of cells were spotted onto poly-L-lysine coated wells for 10 min at 24°C in the humid chamber. Excess solution was aspirated, and the slides were plunged into a coplin jar containing ice-cold methanol for 6 min followed by ice-cold acetone for 30 s. Fixed and permeabilized cells were blocked using Image-iT FX Signal Enhancer (Thermo Fisher, I36933) for 30 min at 24°C in the humid chamber with gentle shaking. Excess solution was aspirated and wells were washed five times with blocking buffer [PBS (pH 7.4), 5% normal goat serum (50062Z, Thermo Fisher), 1% BSA (80055-674, MilliporeSigma) and 2% TritonX-100]. Wells were blocked again with 20 µl blocking buffer for 30 min at 24°C in the humid chamber with gentle shaking. After aspiration, cells were incubated with 20 µl of rabbit anti-p44/42 primary antibody (Cell Signaling Technology, 9101), prepared in blocking buffer at 1:20 dilution for 12 h at 24°C in a humid chamber with gentle shaking. Wells were washed five times for 5 min each with blocking buffer and co-stained with goat anti-rabbit IgG (H+L) Highly Cross-Adsorbed Secondary Antibody, Alexa Fluor 647 (Thermo Fisher, A-21245) and DAPI (4′,6-diamidino-2-phenylindole) at 1:1000 dilution each for 4 h at 24°C in a dark humid chamber with gentle shaking. Wells were washed five times for 10 min each with blocking buffer. After the last wash, wells were sealed with ProLong Diamond Antifade Mountant (Thermo Fisher, P36970) and covered with a cover slip. Slides were incubated in dark at 24°C for 24 h prior to imaging.

Image analysis

The comparison between negative control (no primary antibody), non-inducing (YEPD) and inducing conditions (YEP-GAL) was reported using total fluorescence intensities. The difference between negative control, non-inducing and inducing conditions was at the population level and, therefore, large enough to be measured using total fluorescence intensity values. Briefly, total fluorescent intensity for each cell was measured in ImageJ by subtracting background intensity from the mean fluorescent intensity, which was recorded using Analyze>Measure option. Normalized fluorescent intensity for each cell was quantified as previously described (Okada et al., 2017; Prabhakar et al., 2020) using a custom MATLAB (MATLAB R2016b, The MathWorks) code (Prabhakar et al., 2020). For each cell, pixel intensities greater than the mean+2 standard deviations were background subtracted, normalized to the peak value (which was set to 1) and summed. This value tells us how many pixels in a given cell are two standard deviations brighter than the average pixel intensity in the cell. For the relationship between Sho1p localization and fMAPK induction, the difference in P∼Kss1p signal was compared at the single-cell level under the same growth condition (YEP-GAL), which could not be represented either by total fluorescence intensity or by average fluorescence intensity. Therefore, calculation of normalized fluorescent intensity allowed analysis of biologically relevant differences.

For time-lapse microscopy, raw images were imported into ImageJ. Cells were registered using HyperStackReg plug-in (Thévenaz et al., 1998; Sharma, 2018) to remove drift in the position of cells that occurred during imaging. Grayscale fluorescence images were converted to maximum intensity projection and inverted. Kymographs were performed as described previously (Prabhakar et al., 2020).

Quantitative PCR analysis

Quantitative RT-qPCR was performed as previously described previously (Adhikari and Cullen, 2014; Chow et al., 2019a; Prabhakar et al., 2020). Samples harvested during cell-cycle experiments were used for total RNA extraction, which was carried out using hot acid phenol-chloroform treatment with further purification with the RNeasy Mini Kit (Qiagen, 74104). RNA stability was determined by agarose gel electrophoresis in 0.8% agarose Tris-Borato-EDTA (TBE, 89 mM Tris base, 89 mM boric acid and 2 mM EDTA). Concentration and purity were determined by absorbance using NanoDrop (NanoDrop, 2000C, Thermo Fisher Scientific). Concentration of total RNA was adjusted to 60 ng/µl and cDNA was synthesized using iScript Reverse Transcriptase Supermix (BioRad, 1708840). qPCR was performed using iTaq Universal SYBR Green Supermix (BioRad, 1725120) on a BioRad thermocycler (CFX384 Real-Time System). Reactions contained 10 µl samples (2.5 µl 60 ng/µl cDNA, 0.2 µM each primer and 5 µl SYBR Green master mix). Relative gene expression was calculated using the $2^{-\Delta Ct}$ formula, where Ct is defined as the cycle at which fluorescence was determined to be statistically significant above background; ΔCt is the difference in Ct of the gene of interest and the housekeeping gene (*ACT1*). The primers used were: *MSB2* forward 5′-CACTGCAAGCAGGTGGCTCT-3′; *MSB2* reverse, 5′-GAGGAGCCCGACAGTGTTGC-3′; *HKR1* forward, 5′-AAACCATGGGCGAAAATGGC-3′; *HKR1* reverse, 5′-AAGGCAGGGGCTGTGAATAC-3′; *KSS1* forward, 5′-CCCAAGTGATGAGCCGGAAT-3′; *KSS1* reverse, 5′-TGGGCACTTCTTCCTCCTCT-3′; *SHO1* forward, 5′-AACTACGATGGGAGACACTTTG-3′; *SHO1* reverse, 5′-TCGTAAGCATCATCGTCATCAG-3′ (Adhikari and Cullen, 2014); *TEC1* forward, 5′-ATGTTTCCAGAAGCCGTAGTT-3′; *TEC1* reverse, 5′-TTTAGCACCCAGTCCAGTATTT-3′ (Adhikari and Cullen, 2014); *STE12* forward, 5′-GCAATCTTACCCAAACGGAATG-3′; *STE12* reverse, 5′-AATCGTCCGCGCCATAAA-3′ (Adhikari and Cullen, 2014); *FLO11* forward, 5′-CACTTTTGAAGTTTATGCCACACAAG-3′; *FLO11* reverse, 5′-CTTGCATATTGAGCGGCACTAC-3′ (Chen and Fink, 2006); *ACT1* forward, 5′-TGGATTCCGGTGATGGTGTT-3′; *ACT1* reverse, 5′-CGGCCAAATCGATTCTCAA-3′ (Chow et al., 2019b). Experiments were performed with two independent biological replicates and two technical replicates for each biological replicate.

Statistical analysis

Statistical tests and sample size (*n*) are described in figure legends wherever applicable. Statistical analyses were performed in Microsoft Excel and Minitab (www.minitab.com). One-way ANOVA with Tukey's test and/or Dunnett's test was used for statistical analysis.

Acknowledgements

We thank Haruo Saito (University of Tokyo) for reagents and Andrew Pitoniak for help with experiments.

Competing interests
The authors declare no competing or financial interests.

Author contributions
Conceptualization: A.P., H.D., P.C.; Methodology: A.P.; Validation: A.P.; Investigation: A.P., B.G., S.B., P.C.; Data curation: A.P.; Writing - original draft: A.P., P.C.; Writing - review & editing: A.P., P.C.; Visualization: A.P.; Supervision: P.C.

Funding
This work was supported by a grant from the National Institute of General Medical Sciences (GM#098629). Deposited in PMC for release after 12 months.

Peer review history
The peer review history is available online at https://journals.biologists.com/jcs/article-lookup/doi/10.1242/jcs.258341

References

Acharya, U., Mallabiabarrena, A., Acharya, J. K. and Malhotra, V. (1998). Signaling via mitogen-activated protein kinase kinase (MEK1) is required for Golgi fragmentation during mitosis. *Cell* **92**, 183-192. doi:10.1016/S0092-8674(00)80913-7

Adhikari, H. and Cullen, P. J. (2014). Metabolic respiration induces AMPK- and Ire1p-dependent activation of the p38-Type HOG MAPK pathway. *PLoS Genet.* **10**, e1004734. doi:10.1371/journal.pgen.1004734

Adhikari, H., Caccamise, L. M., Pande, T. and Cullen, P. J. (2015a). Comparative analysis of transmembrane regulators of the filamentous growth mitogen-activated protein kinase pathway uncovers functional and regulatory differences. *Eukaryot. Cell* **14**, 868-883. doi:10.1128/EC.00085-15

Adhikari, H., Vadaie, N., Chow, J., Caccamise, L. M., Chavel, C. A., Li, B., Bowitch, A., Stefan, C. J. and Cullen, P. J. (2015b). Role of the unfolded protein response in regulating the mucin-dependent filamentous-growth mitogen-activated protein kinase pathway. *Mol. Cell. Biol.* **35**, 1414-1432. doi:10.1128/MCB.01501-14

Ahn, S. H., Acurio, A. and Kron, S. J. (1999). Regulation of G2/M progression by the STE mitogen-activated protein kinase pathway in budding yeast filamentous growth. *Mol. Biol. Cell* **10**, 3301-3316. doi:10.1091/mbc.10.10.3301

Aktas, H., Cai, H. and Cooper, G. M. (1997). Ras links growth factor signaling to the cell cycle machinery via regulation of cyclin D1 and the Cdk inhibitor p27KIP1. *Mol. Cell. Biol.* **17**, 3850-3857. doi:10.1128/MCB.17.7.3850

Amberg, D. C., Burke, D. J. and Strathern, J. N. (2006). Yeast immunofluorescence. *Cold Spring Harb. Protoc.* **2006**, pdb.prot4167. doi:10.1101/pdb.prot4167

Andrews, B. J. and Herskowitz, I. (1989). The yeast SWI4 protein contains a motif present in developmental regulators and is part of a complex involved in cell-cycle-dependent transcription. *Nature* **342**, 830-833. doi:10.1038/342830a0

Bardwell, L. (2004). A walk-through of the yeast mating pheromone response pathway. *Peptides* **25**, 1465-1476. doi:10.1016/j.peptides.2003.10.022

Bardwell, L. (2006). Mechanisms of MAPK signalling specificity. *Biochem. Soc. Trans.* **34**, 837-841. doi:10.1042/BST0340837

Bardwell, L., Cook, J. G., Chang, E. C., Cairns, B. R. and Thorner, J. (1996). Signaling in the yeast pheromone response pathway: specific and high-affinity interaction of the mitogen-activated protein (MAP) kinases Kss1 and Fus3 with the upstream MAP kinase kinase Ste7. *Mol. Cell. Biol.* **16**, 3637-3650. doi:10.1128/MCB.16.7.3637

Bardwell, L., Cook, J. G., Voora, D., Baggott, D. M., Martinez, A. R. and Thorner, J. (1998). Repression of yeast Ste12 transcription factor by direct binding of unphosphorylated Kss1 MAPK and its regulation by the Ste7 MEK. *Genes Dev.* **12**, 2887-2898. doi:10.1101/gad.12.18.2887

Basu, S., Vadaie, N., Prabhakar, A., Li, B., Adhikari, H., Pitoniak, A., Chow, J., Chavel, C. A. and Cullen, P. J. (2016). Spatial landmarks regulate a Cdc42-dependent MAPK pathway to control differentiation and the response to positional compromise. *Proc. Natl. Acad. Sci. USA* **113**, E2019-E2028. doi:10.1073/pnas.1522679113

Bi, E. and Park, H.-O. (2012). Cell polarization and cytokinesis in budding yeast. *Genetics* **191**, 347-387. doi:10.1534/genetics.111.132886

Breeden, L. L. (1997). α-Factor synchronization of budding yeast. In *Methods in Enzymology* (ed. Dunphy, W.G.), pp. 332-342. Academic Press.

Breeden, L. and Nasmyth, K. (1987). Cell cycle control of the yeast HO gene: cis- and trans-acting regulators. *Cell* **48**, 389-397. doi:10.1016/0092-8674(87)90190-5

Breitkreutz, A. and Tyers, M. (2002). MAPK signaling specificity: it takes two to tango. *Trends Cell Biol.* **12**, 254-257. doi:10.1016/S0962-8924(02)02284-5

Breker, M., Gymrek, M. and Schuldiner, M. (2013). A novel single-cell screening platform reveals proteome plasticity during yeast stress responses. *J. Cell Biol.* **200**, 839-850. doi:10.1083/jcb.201301120

Brewster, J. L., De Valoir, T., Dwyer, N. D., Winter, E. and Gustin, M. C. (1993). An osmosensing signal transduction pathway in yeast. *Science* **259**, 1760-1763. doi:10.1126/science.7681220

Cao, J.-N., Shafee, N., Vickery, L., Kaluz, S., Ru, N. and Stanbridge, E. J. (2010). Mitogen-activated protein/extracellular signal-regulated kinase kinase 1^{act}/tubulin interaction is an important determinant of mitotic stability in cultured HT1080 human fibrosarcoma cells. *Cancer Res.* **70**, 6004-6014. doi:10.1158/0008-5472.CAN-09-4490

Carlson, M. and Botstein, D. (1982). Two differentially regulated mRNAs with different 5′ ends encode secreted and intracellular forms of yeast invertase. *Cell* **28**, 145-154. doi:10.1016/0092-8674(82)90384-1

Cepeda-García, C. (2017). Determination of cell cycle stage and mitotic exit through the quantification of the protein levels of known mitotic regulators. *Methods Mol. Biol.* **1505**, 45-57. doi:10.1007/978-1-4939-6502-1_4

Cha, H. and Shapiro, P. (2001). Tyrosine-phosphorylated extracellular signal–regulated kinase associates with the Golgi complex during G2/M phase of the cell cycle: evidence for regulation of Golgi structure. *J. Cell Biol.* **153**, 1355-1368. doi:10.1083/jcb.153.7.1355

Chant, J., Mischke, M., Mitchell, E., Herskowitz, I. and Pringle, J. R. (1995). Role of Bud3p in producing the axial budding pattern of yeast. *J. Cell Biol.* **129**, 767-778. doi:10.1083/jcb.129.3.767

Chavel, C. A., Dionne, H. M., Birkaya, B., Joshi, J. and Cullen, P. J. (2010). Multiple signals converge on a differentiation MAPK pathway. *PLoS Genet.* **6**, e1000883. doi:10.1371/journal.pgen.1000883

Chen, H. and Fink, G. R. (2006). Feedback control of morphogenesis in fungi by aromatic alcohols. *Genes Dev.* **20**, 1150-1161. doi:10.1101/gad.1411806

Chen, R. E. and Thorner, J. (2007). Function and regulation in MAPK signaling pathways: lessons learned from the yeast Saccharomyces cerevisiae. *Biochim. Biophys. Acta (BBA) Mol. Cell Res.* **1773**, 1311-1340. doi:10.1016/j.bbamcr.2007.05.003

Chen, R. H., Sarnecki, C. and Blenis, J. (1992). Nuclear localization and regulation of erk- and rsk-encoded protein kinases. *Mol. Cell Biol.* **12**, 915-927.

Cho, R. J., Campbell, M. J., Winzeler, E. A., Steinmetz, L., Conway, A., Wodicka, L., Wolfsberg, T. G., Gabrielian, A. E., Landsman, D., Lockhart, D. J. et al. (1998). A genome-wide transcriptional analysis of the mitotic cell cycle. *Mol. Cell* **2**, 65-73. doi:10.1016/S1097-2765(00)80114-8

Chow, J., Dionne, H. M., Prabhakar, A., Mehrotra, A., Somboonthum, J., Gonzalez, B., Edgerton, M. and Cullen, P. J. (2019a). Aggregate filamentous growth responses in yeast. *mSphere* **4**, e00702-e00718. doi:10.1128/mSphere.00702-18

Chow, J., Starr, I., Jamalzadeh, S., Muniz, O., Kumar, A., Gokcumen, O., Ferkey, D. M. and Cullen, P. J. (2019b). Filamentation regulatory pathways control adhesion-dependent surface responses in yeast. *Genetics* **212**, 667-690. doi:10.1534/genetics.119.302004

Cook, J. G., Bardwell, L. and Thorner, J. (1997). Inhibitory and activating functions for MAPK Kss1 in the *S. cerevisiae* filamentous- growth signalling pathway. *Nature* **390**, 85-88. doi:10.1038/36355

Cullen, P. J. and Sprague, G. F.Jr. (2000). Glucose depletion causes haploid invasive growth in yeast. *Proc. Natl. Acad. Sci. USA* **97**, 13619-13624. doi:10.1073/pnas.240345197

Cullen, P. J. and Sprague, G. F.Jr. (2002). The roles of bud-site-selection proteins during haploid invasive growth in yeast. *Mol. Biol. Cell* **13**, 2990-3004. doi:10.1091/mbc.e02-03-0151

Cullen, P. J., Schultz, J., Horecka, J., Stevenson, B. J., Jigami, Y. and Sprague, G. F. (2000). Defects in protein glycosylation cause SHO1- dependent activation of a STE12 signaling pathway in yeast. *Genetics* **155**, 1005-1018. doi:10.1093/genetics/155.3.1005

Cullen, P. J., Sabbagh, W., Jr., Graham, E., Irick, M. M., Van Olden, E. K., Neal, C., Delrow, J., Bardwell, L. and Sprague, G. F.Jr. (2004). A signaling mucin at the head of the Cdc42- and MAPK-dependent filamentous growth pathway in yeast. *Genes Dev.* **18**, 1695-1708. doi:10.1101/gad.1178604

Dangi, S., Chen, F. M. and Shapiro, P. (2006). Activation of extracellular signal-regulated kinase (ERK) in G2 phase delays mitotic entry through p21CIP1. *Cell Prolif.* **39**, 261-279. doi:10.1111/j.1365-2184.2006.00388.x

Davenport, K. D., Williams, K. E., Ullmann, B. D. and Gustin, M. C. (1999). Activation of the Saccharomyces cerevisiae filamentation/invasion pathway by osmotic stress in high-osmolarity glycogen pathway mutants. *Genetics* **153**, 1091-1103. doi:10.1093/genetics/153.3.1091

De Vit, M. J., Waddle, J. A. and Johnston, M. (1997). Regulated nuclear translocation of the Mig1 glucose repressor. *Mol. Biol. Cell* **8**, 1603-1618. doi:10.1091/mbc.8.8.1603

Dinsmore, C. J. and Soriano, P. (2018). MAPK and PI3K signaling: at the crossroads of neural crest development. *Dev. Biol.* **444** Suppl. 1, S79-S97. doi:10.1016/j.ydbio.2018.02.003

Elion, E. A., Satterberg, B. and Kranz, J. E. (1993). FUS3 phosphorylates multiple components of the mating signal transduction cascade: evidence for STE12 and FAR1. *Mol. Biol. Cell* **4**, 495-510. doi:10.1091/mbc.4.5.495

Eluère, R., Offner, N., Varlet, I., Motteux, O., Signon, L., Picard, A., Bailly, E. and Simon, M.-N. (2007). Compartmentalization of the functions and regulation of the mitotic cyclin Clb2 in *S. cerevisiae*. *J. Cell Sci.* **120**, 702-711. doi:10.1242/jcs.03380

Escoté, X., Zapater, M., Clotet, J. and Posas, F. (2004). Hog1 mediates cell-cycle arrest in G1 phase by the dual targeting of Sic1. *Nat. Cell Biol.* **6**, 997-1002. doi:10.1038/ncb1174

Fischer, M. S., Wu, V. W., Lee, J. E., O'malley, R. C. and Glass, N. L. (2018). Regulation of cell-to-cell communication and cell wall integrity by a network of MAP kinase pathways and transcription factors in *Neurospora crassa*. *Genetics* **209**, 489-506. doi:10.1534/genetics.118.300904

Gancedo, J. M. (2001). Control of pseudohyphae formation in *Saccharomyces cerevisiae*. *FEMS Microbiol. Rev.* **25**, 107-123. doi:10.1111/j.1574-6976.2001.tb00573.x

Gimeno, C. J., Ljungdahl, P. O., Styles, C. A. and Fink, G. R. (1992). Unipolar cell divisions in the yeast S. cerevisiae lead to filamentous growth: regulation by starvation and RAS. *Cell* **68**, 1077-1090. doi:10.1016/0092-8674(92)90079-R

Goldstein, A. L. and Mccusker, J. H. (1999). Three new dominant drug resistance cassettes for gene disruption in *Saccharomyces cerevisiae*. *Yeast* **15**, 1541-1553. doi:10.1002/(SICI)1097-0061(199910)15:14<1541::AID-YEA476>3.0.CO;2-K

Guo, B., Styles, C. A., Feng, Q. and Fink, G. R. (2000). A Saccharomyces gene family involved in invasive growth, cell-cell adhesion, and mating. *Proc. Natl. Acad. Sci. USA* **97**, 12158-12163. doi:10.1073/pnas.220420397

Hall, P. A., Hilary, S. E., Russell, H. and Pringle, J. R. (2008). *The Septins*. Wiley-Blackwell.

Hao, N., Zeng, Y., Elston, T. C. and Dohlman, H. G. (2008). Control of MAPK specificity by feedback phosphorylation of shared adaptor protein Ste50. *J. Biol. Chem.* **283**, 33798-33802. doi:10.1074/jbc.C800179200

Harkins, H. A., Pagé, N., Schenkman, L. R., De Virgilio, C., Shaw, S., Bussey, H. and Pringle, J. R. (2001). Bud8p and Bud9p, proteins that may mark the sites for bipolar budding in yeast. *Mol. Biol. Cell* **12**, 2497-2518. doi:10.1091/mbc.12.8.2497

Hirosumi, J., Tuncman, G., Chang, L., Görgün, C. Z., Uysal, K. T., Maeda, K., Karin, M. and Hotamisligil, G. S. (2002). A central role for JNK in obesity and insulin resistance. *Nature* **420**, 333-336. doi:10.1038/nature01137

Horne, M. M. and Guadagno, T. M. (2003). A requirement for MAP kinase in the assembly and maintenance of the mitotic spindle. *J. Cell Biol.* **161**, 1021-1028. doi:10.1083/jcb.200304144

Ingram, A. J., James, L., Cai, L., Thai, K., Ly, H. and Scholey, J. W. (2000). NO inhibits stretch-induced MAPK activity by cytoskeletal disruption. *J. Biol. Chem.* **275**, 40301-40306. doi:10.1074/jbc.M007018200

Iyer, V. R., Horak, C. E., Scafe, C. S., Botstein, D., Snyder, M. and Brown, P. O. (2001). Genomic binding sites of the yeast cell-cycle transcription factors SBF and MBF. *Nature* **409**, 533-538. doi:10.1038/35054095

Johnson, D. I. (1999). Cdc42: an essential Rho-type GTPase controlling eukaryotic cell polarity. *Microbiol. Mol. Biol. Rev.* **63**, 54-105. doi:10.1128/MMBR.63.1.54-105.1999

Johnson, G. L. and Lapadat, R. (2002). Mitogen-activated protein kinase pathways mediated by ERK, JNK, and p38 protein kinases. *Science* **298**, 1911-1912. doi:10.1126/science.1072682

Jordan, J. D., Landau, E. M. and Iyengar, R. (2000). Signaling networks: the origins of cellular multitasking. *Cell* **103**, 193-200. doi:10.1016/S0092-8674(00)00112-4

Karunanithi, S. and Cullen, P. J. (2012). The filamentous growth MAPK pathway responds to glucose starvation through the Mig1/2 transcriptional repressors in *Saccharomyces cerevisiae*. *Genetics* **192**, 869-887. doi:10.1534/genetics.112.142661

Katz, M., Amit, I. and Yarden, Y. (2007). Regulation of MAPKs by growth factors and receptor tyrosine kinases. *Biochim. Biophys. Acta (BBA) Mol. Cell Res.* **1773**, 1161-1176. doi:10.1016/j.bbamcr.2007.01.002

Kim, H. B., Haarer, B. K. and Pringle, J. R. (1991). Cellular morphogenesis in the *Saccharomyces cerevisiae* cell cycle: localization of the CDC3 gene product and the timing of events at the budding site. *J. Cell Biol.* **112**, 535-544. doi:10.1083/jcb.112.4.535

Koç, A., Wheeler, L. J., Mathews, C. K. and Merrill, G. F. (2004). Hydroxyurea arrests DNA replication by a mechanism that preserves basal dNTP pools. *J. Biol. Chem.* **279**, 223-230. doi:10.1074/jbc.M303952200

Kuczera, T., Bayram, Ö., Sari, F., Braus, G. H. and Irniger, S. (2010). Dissection of mitotic functions of the yeast cyclin Clb2. *Cell Cycle* **9**, 2611-2619. doi:10.4161/cc.9.13.12082

Labedzka, K., Tian, C., Nussbaumer, U., Timmermann, S., Walther, P., Müller, J. and Johnsson, N. (2012). Sho1p connects the plasma membrane with proteins of the cytokinesis network through multiple isomeric interaction states. *J. Cell Sci.* **125**, 4103-4113. doi:10.1242/jcs.105320

Lavoie, H., Gagnon, J. and Therrien, M. (2020). ERK signalling: a master regulator of cell behaviour, life and fate. *Nat. Rev. Mol. Cell Biol.* **21**, 607-632. doi:10.1038/s41580-020-0255-7

Lawrence, M. C., Jivan, A., Shao, C., Duan, L., Goad, D., Zaganjor, E., Osborne, J., Mcglynn, K., Stippec, S., Earnest, S. et al. (2008). The roles of MAPKs in disease. *Cell Res.* **18**, 436-442. doi:10.1038/cr.2008.37

Leberer, E., Wu, C., Leeuw, T., Fourest-Lieuvin, A., Segall, J. E. and Thomas, D. Y. (1997). Functional characterization of the Cdc42p binding domain of yeast Ste20p protein kinase. *EMBO J.* **16**, 83-97. doi:10.1093/emboj/16.1.83

Lee, M. J. and Dohlman, H. G. (2008). Coactivation of G protein signaling by cell-surface receptors and an intracellular exchange factor. *Curr. Biol.* **18**, 211-215. doi:10.1016/j.cub.2008.01.007

Lee, K. S., Irie, K., Gotoh, Y., Watanabe, Y., Araki, H., Nishida, E., Matsumoto, K. and Levin, D. E. (1993). A yeast mitogen-activated protein kinase homolog (Mpk1p) mediates signalling by protein kinase C. *Mol. Cell Biol.* **13**, 3067-3075.

Lee, J. C., Kumar, S., Griswold, D. E., Underwood, D. C., Votta, B. J. and Adams, J. L. (2000). Inhibition of p38 MAP kinase as a therapeutic strategy. *Immunopharmacology* **47**, 185-201. doi:10.1016/S0162-3109(00)00206-X

Lenormand, P., Sardet, C., Pagès, G., L'allemain, G., Brunet, A. and Pouysségur, J. (1993). Growth factors induce nuclear translocation of MAP kinases (p42mapk and p44mapk) but not of their activator MAP kinase kinase (p45mapkk) in fibroblasts. *J. Cell Biol.* **122**, 1079-1088. doi:10.1083/jcb.122.5.1079

Leone, G., Degregori, J., Sears, R., Jakoi, L. and Nevins, J. R. (1997). Myc and Ras collaborate in inducing accumulation of active cyclin E/Cdk2 and E2F. *Nature* **387**, 422-426. doi:10.1038/387422a0

Lippincott, J., Shannon, K. B., Shou, W., Deshaies, R. J. and Li, R. (2001). The Tem1 small GTPase controls actomyosin and septin dynamics during cytokinesis. *J. Cell Sci.* **114**, 1379-1386. doi:10.1242/jcs.114.7.1379

Lo, H.-J., Köhler, J. R., Didomenico, B., Loebenberg, D., Cacciapuoti, A. and Fink, G. R. (1997). Nonfilamentous C. albicans mutants are avirulent. *Cell* **90**, 939-949. doi:10.1016/S0092-8674(00)80358-X

Loeb, J. D., Kerentseva, T. A., Pan, T., Sepulveda-Becerra, M. and Liu, H. (1999). Saccharomyces cerevisiae G1 cyclins are differentially involved in invasive and pseudohyphal growth independent of the filamentation mitogen-activated protein kinase pathway. *Genetics* **153**, 1535-1546. doi:10.1093/genetics/153.4.1535

Longtine, M. S., Mckenzie, A., III, Demarini, D. J., Shah, N. G., Wach, A., Brachat, A., Philippsen, P. and Pringle, J. R. (1998). Additional modules for versatile and economical PCR-based gene deletion and modification in Saccharomyces cerevisiae. *Yeast* **14**, 953-961. doi:10.1002/(SICI)1097-0061(199807)14:10<953::AID-YEA293>3.0.CO;2-U

Ma, D., Cook, J. G. and Thorner, J. (1995). Phosphorylation and localization of Kss1, a MAP kinase of the Saccharomyces cerevisiae pheromone response pathway. *Mol. Biol. Cell* **6**, 889-909. doi:10.1091/mbc.6.7.889

Macisaac, K. D., Wang, T., Gordon, D. B., Gifford, D. K., Stormo, G. D. and Fraenkel, E. (2006). An improved map of conserved regulatory sites for *Saccharomyces cerevisiae*. *BMC Bioinform.* **7**, 113. doi:10.1186/1471-2105-7-113

Madhani, H. D. and Fink, G. R. (1997). Combinatorial control required for the specificity of yeast MAPK signaling. *Science* **275**, 1314-1317. doi:10.1126/science.275.5304.1314

Madhani, H. D., Styles, C. A. and Fink, G. R. (1997). MAP kinases with distinct inhibitory functions impart signaling specificity during yeast differentiation. *Cell* **91**, 673-684. doi:10.1016/S0092-8674(00)80454-7

Madhani, H. D., Galitski, T., Lander, E. S. and Fink, G. R. (1999). Effectors of a developmental mitogen-activated protein kinase cascade revealed by expression signatures of signaling mutants. *Proc. Natl. Acad. Sci. USA* **96**, 12530-12535. doi:10.1073/pnas.96.22.12530

Maeda, T., Wurgler-Murphy, S. M. and Saito, H. (1994). A two-component system that regulates an osmosensing MAP kinase cascade in yeast. *Nature* **369**, 242-245. doi:10.1038/369242a0

Maekawa, M., Yamamoto, T., Tanoue, T., Yuasa, Y., Chisaka, O. and Nishida, E. (2005). Requirement of the MAP kinase signaling pathways for mouse preimplantation development. *Development* **132**, 1773-1783. doi:10.1242/dev.01729

Mansour, S. J., Matten, W. T., Hermann, A. S., Candia, J. M., Rong, S., Fukasawa, K., Vande Woude, G. and Ahn, N. G. (1994). Transformation of mammalian cells by constitutively active MAP kinase kinase. *Science* **265**, 966-970. doi:10.1126/science.8052857

Marles, J. A., Dahesh, S., Haynes, J., Andrews, B. J. and Davidson, A. R. (2004). Protein-protein interaction affinity plays a crucial role in controlling the Sho1p-mediated signal transduction pathway in yeast. *Mol. Cell* **14**, 813-823. doi:10.1016/j.molcel.2004.05.024

Mccaffrey, G., Clay, F. J., Kelsay, K. and Sprague, G. F.Jr. (1987). Identification and regulation of a gene required for cell fusion during mating of the yeast Saccharomyces cerevisiae. *Mol. Cell Biol.* **7**, 2680-2690.

Mcmurray, M. A. and Thorner, J. (2009). Septins: molecular partitioning and the generation of cellular asymmetry. *Cell Div.* **4**, 18. doi:10.1186/1747-1028-4-18

Meitinger, F., Boehm, M. E., Hofmann, A., Hub, B., Zentgraf, H., Lehmann, W. D. and Pereira, G. (2011). Phosphorylation-dependent regulation of the F-BAR protein Hof1 during cytokinesis. *Genes Dev.* **25**, 875-888. doi:10.1101/gad.622411

Meitinger, F., Palani, S., Hub, B. and Pereira, G. (2013). Dual function of the NDR-kinase Dbf2 in the regulation of the F-BAR protein Hof1 during cytokinesis. *Mol. Biol. Cell* **24**, 1290-1304. doi:10.1091/mbc.e12-08-0608

Molgaard, S., Ulrichsen, M., Olsen, D. and Glerup, S. (2016). Detection of phosphorylated Akt and MAPK in cell culture assays. *MethodsX* **3**, 386-398. doi:10.1016/j.mex.2016.04.009

Mosch, H. U., Roberts, R. L. and Fink, G. R. (1996). Ras2 signals via the Cdc42/Ste20/mitogen-activated protein kinase module to induce filamentous growth in Saccharomyces cerevisiae. *Proc. Natl. Acad. Sci. USA* **93**, 5352-5356. doi:10.1073/pnas.93.11.5352

Nagiec, M. J. and Dohlman, H. G. (2012). Checkpoints in a yeast differentiation pathway coordinate signaling during hyperosmotic stress. *PLoS Genet.* **8**, e1002437. doi:10.1371/journal.pgen.1002437

Nasmyth, K. and Dirick, L. (1991). The role of SWI4 and SWI6 in the activity of G1 cyclins in yeast. *Cell* **66**, 995-1013. doi:10.1016/0092-8674(91)90444-4

Nehlin, J. O., Carlberg, M. and Ronne, H. (1991). Control of yeast GAL genes by MIG1 repressor: a transcriptional cascade in the glucose response. *EMBO J.* **10**, 3373-3377. doi:10.1002/j.1460-2075.1991.tb04901.x

Nelson, B., Parsons, A. B., Evangelista, M., Schaefer, K., Kennedy, K., Ritchie, S., Petryshen, T. L. and Boone, C. (2004). Fus1p interacts with components of the Hog1p mitogen-activated protein kinase and Cdc42p morphogenesis signaling pathways to control cell fusion during yeast mating. *Genetics* **166**, 67-77. doi:10.1534/genetics.166.1.67

Niu, W., Hart, G. T. and Marcotte, E. M. (2011). High-throughput immunofluorescence microscopy using yeast spheroplast cell-based microarrays. *Methods Mol. Biol.* **706**, 83-95. doi:10.1007/978-1-61737-970-3_7

Oh, Y., Schreiter, J., Nishihama, R., Wloka, C. and Bi, E. (2013). Targeting and functional mechanisms of the cytokinesis-related F-BAR protein Hof1 during the cell cycle. *Mol. Biol. Cell* **24**, 1305-1320. doi:10.1091/mbc.e12-11-0804

Okada, S., Lee, M. E., Bi, E. and Park, H.-O. (2017). Probing Cdc42 polarization dynamics in budding yeast using a biosensor. *Methods Enzymol.* **589**, 171-190. doi:10.1016/bs.mie.2017.01.011

Omori, S., Hida, M., Fujita, H., Takahashi, H., Tanimura, S., Kohno, M. and Awazu, M. (2006). Extracellular signal-regulated kinase inhibition slows disease progression in mice with polycystic kidney disease. *J. Am. Soc. Nephrol.* **17**, 1604-1614. doi:10.1681/ASN.2004090800

O'Rourke, S. M. and Herskowitz, I. (1998). The Hog1 MAPK prevents cross talk between the HOG and pheromone response MAPK pathways in Saccharomyces cerevisiae. *Genes Dev.* **12**, 2874-2886. doi:10.1101/gad.12.18.2874

O'Rourke, S. M. and Herskowitz, I. (2002). A third osmosensing branch in Saccharomyces cerevisiae requires the Msb2 protein and functions in parallel with the Sho1 branch. *Mol. Cell. Biol.* **22**, 4739-4749. doi:10.1128/MCB.22.13.4739-4749.2002

Ostrow, A. Z., Nellimoottil, T., Knott, S. R. V., Fox, C. A., Tavaré, S. and Aparicio, O. M. (2014). Fkh1 and Fkh2 bind multiple chromosomal elements in the S. cerevisiae genome with distinct specificities and cell cycle dynamics. *PLoS ONE* **9**, e87647. doi:10.1371/journal.pone.0087647

Pagès, G., Lenormand, P., L'allemain, G., Chambard, J. C., Meloche, S. and Pouyssegur, J. (1993). Mitogen-activated protein kinases p42mapk and p44mapk are required for fibroblast proliferation. *Proc. Natl. Acad. Sci. USA* **90**, 8319-8323. doi:10.1073/pnas.90.18.8319

Pan, X., Harashima, T. and Heitman, J. (2000). Signal transduction cascades regulating pseudohyphal differentiation of Saccharomyces cerevisiae. *Curr. Opin. Microbiol.* **3**, 567-572. doi:10.1016/S1369-5274(00)00142-9

Papa, S., Choy, P. M. and Bubici, C. (2019). The ERK and JNK pathways in the regulation of metabolic reprogramming. *Oncogene* **38**, 2223-2240. doi:10.1038/s41388-018-0582-8

Pelet, S. (2017). Nuclear relocation of Kss1 contributes to the specificity of the mating response. *Sci. Rep.* **7**, 43636. doi:10.1038/srep43636

Peter, M. and Herskowitz, I. (1994). Direct inhibition of the yeast cyclin-dependent kinase Cdc28-Cln by Far1. *Science* **265**, 1228-1231. doi:10.1126/science.8066461

Peter, M., Gartner, A., Horecka, J., Ammerer, G. and Herskowitz, I. (1993). FAR1 links the signal transduction pathway to the cell cycle machinery in yeast. *Cell* **73**, 747-760. doi:10.1016/0092-8674(93)90254-N

Peter, M., Neiman, A. M., Park, H. O., Van Lohuizen, M. and Herskowitz, I. (1996). Functional analysis of the interaction between the small GTP binding protein Cdc42 and the Ste20 protein kinase in yeast. *EMBO J.* **15**, 7046-7059. doi:10.1002/j.1460-2075.1996.tb01096.x

Pitoniak, A., Birkaya, B., Dionne, H. M., Vadaie, N. and Cullen, P. J. (2009). The signaling mucins Msb2 and Hkr1 differentially regulate the filamentation mitogen-activated protein kinase pathway and contribute to a multimodal response. *Mol. Biol. Cell* **20**, 3101-3114. doi:10.1091/mbc.e08-07-0760

Pitoniak, A., Chavel, C. A., Chow, J., Smith, J., Camara, D., Karunanithi, S., Li, B., Wolfe, K. H. and Cullen, P. J. (2015). Cdc42p-interacting protein Bem4p regulates the filamentous-growth mitogen-activated protein kinase pathway. *Mol. Cell. Biol.* **35**, 417-436. doi:10.1128/MCB.00850-14

Posas, F. and Saito, H. (1997). Osmotic activation of the HOG MAPK pathway via Ste11p MAPKKK: scaffold role of Pbs2p MAPKK. *Science* **276**, 1702-1705. doi:10.1126/science.276.5319.1702

Pouysségur, J., Volmat, V. and Lenormand, P. (2002). Fidelity and spatio-temporal control in MAP kinase (ERKs) signalling. *Biochem. Pharmacol.* **64**, 755-763. doi:10.1016/S0006-2952(02)01135-8

Prabhakar, A., Vadaie, N., Krzystek, T. and Cullen, P. J. (2019). Proteins that interact with the mucin-type Glycoprotein Msb2p include a regulator of the actin cytoskeleton. *Biochemistry* **58**, 4842-4856. doi:10.1021/acs.biochem.9b00725

Prabhakar, A., Chow, J., Siegel, A. J. and Cullen, P. J. (2020). Regulation of intrinsic polarity establishment by a differentiation-type MAPK pathway. *J. Cell Sci* **133**, jcs241513. doi:10.1242/jcs.241513

Radmaneshfar, E., Kaloriti, D., Gustin, M. C., Gow, N. A. R., Brown, A. J., Grebogi, C., Romano, M. C. and Thiel, M. (2013). From START to FINISH: the influence of osmotic stress on the cell cycle. *PLoS ONE* **8**, e68067. doi:10.1371/journal.pone.0068067

Raitt, D. C., Posas, F. and Saito, H. (2000). Yeast Cdc42 GTPase and Ste20 PAK-like kinase regulate Sho1-dependent activation of the Hog1 MAPK pathway. *EMBO J.* **19**, 4623-4631. doi:10.1093/emboj/19.17.4623

Raman, M., Chen, W. and Cobb, M. H. (2007). Differential regulation and properties of MAPKs. *Oncogene* **26**, 3100-3112. doi:10.1038/sj.onc.1210392

Reiser, V., Raitt, D. C. and Saito, H. (2003). Yeast osmosensor Sln1 and plant cytokinin receptor Cre1 respond to changes in turgor pressure. *J. Cell Biol.* **161**, 1035-1040. doi:10.1083/jcb.200301099

Richardson, H., Lew, D. J., Henze, M., Sugimoto, K. and Reed, S. I. (1992). Cyclin-B homologs in Saccharomyces cerevisiae function in S phase and in G2. *Genes Dev.* **6**, 2021-2034. doi:10.1101/gad.6.11.2021

Roberts, P. J. and Der, C. J. (2007). Targeting the Raf-MEK-ERK mitogen-activated protein kinase cascade for the treatment of cancer. *Oncogene* **26**, 3291-3310. doi:10.1038/sj.onc.1210422

Roberts, R. L. and Fink, G. R. (1994). Elements of a single MAP kinase cascade in Saccharomyces cerevisiae mediate two developmental programs in the same cell type: mating and invasive growth. *Genes Dev.* **8**, 2974-2985. doi:10.1101/gad.8.24.2974

Roberts, C. J., Nelson, B., Marton, M. J., Stoughton, R., Meyer, M. R., Bennett, H. A., He, Y. D., Dai, H., Walker, W. L. and Hughes, T. R. (2000). Signaling and circuitry of multiple MAPK pathways revealed by a matrix of global gene expression profiles. *Science* **287**, 873-880. doi:10.1126/science.287.5454.873

Roberts, E. C., Shapiro, P. S., Nahreini, T. S., Pages, G., Pouyssegur, J. and Ahn, N. G. (2002). Distinct cell cycle timing requirements for extracellular signal-regulated kinase and phosphoinositide 3-kinase signaling pathways in somatic cell mitosis. *Mol. Cell. Biol.* **22**, 7226-7241. doi:10.1128/MCB.22.20.7226-7241.2002

Rodriguez-Viciana, P., Tetsu, O., Tidyman, W. E., Estep, A. L., Conger, B. A., Cruz, M. S., McCormick, F. and Rauen, K. A. (2006). Germline mutations in genes within the MAPK pathway cause cardio-facio-cutaneous syndrome. *Science* **311**, 1287-1290. doi:10.1126/science.1124642

Rose, M. D., Winston, F. and Hieter, P. (1990). *Methods in Yeast Genetics*. NY: Cold Spring Harbor Laboratory Press, Cold Spring Harbor.

Rosebrock, A. P. (2017). Synchronization of budding yeast by centrifugal elutriation. *Cold Spring Harb. Protoc.* 2017. doi:10.1101/pdb.prot088732

Rosner, M. R. (2007). MAP kinase meets mitosis: a role for Raf Kinase inhibitory protein in spindle checkpoint regulation. *Cell Div.* **2**, 1. doi:10.1186/1747-1028-2-1

Roux, P. P. and Blenis, J. (2004). ERK and p38 MAPK-activated protein kinases: a family of protein kinases with diverse biological functions. *Microbiol. Mol. Biol. Rev.* **68**, 320-344. doi:10.1128/MMBR.68.2.320-344.2004

Rua, D., Tobe, B. T. and Kron, S. J. (2001). Cell cycle control of yeast filamentous growth. *Curr. Opin. Microbiol.* **4**, 720-727. doi:10.1016/S1369-5274(01)00274-0

Rupp, S., Summers, E., Lo, H.-J., Madhani, H. and Fink, G. (1999). MAP kinase and cAMP filamentation signaling pathways converge on the unusually large promoter of the yeast FLO11 gene. *EMBO J.* **18**, 1257-1269. doi:10.1093/emboj/18.5.1257

Sabbagh, W., Flatauer, L. J., Bardwell, A. J. and Bardwell, L. (2001). Specificity of MAP Kinase signaling in yeast differentiation involves transient versus sustained MAPK activation. *Mol. Cell* **8**, 683-691. doi:10.1016/S1097-2765(01)00322-7

Sambrook, J., Fritsch, E. F. and Maniatis, T. (1989). *Molecular Cloning: A Laboratory Manual*, NY: Cold Spring Harbor Laboratory Press, Cold Spring Harbor.

Sanders, S. L. and Herskowitz, I. (1996). The BUD4 protein of yeast, required for axial budding, is localized to the mother/BUD neck in a cell cycle-dependent manner. *J. Cell Biol.* **134**, 413-427. doi:10.1083/jcb.134.2.413

Schenkman, L. R., Caruso, C., Pagé, N. and Pringle, J. R. (2002). The role of cell cycle-regulated expression in the localization of spatial landmark proteins in yeast. *J. Cell Biol.* **156**, 829-841. doi:10.1083/jcb.200107041

Schneider, B. L., Seufert, W., Steiner, B., Yang, Q. H. and Futcher, A. B. (1995). Use of polymerase chain reaction epitope tagging for protein tagging in *Saccharomyces cerevisiae*. *Yeast* **11**, 1265-1274. doi:10.1002/yea.320111306

Schnell, U., Dijk, F., Sjollema, K. A. and Giepmans, B. N. G. (2012). Immunolabeling artifacts and the need for live-cell imaging. *Nat. Methods* **9**, 152-158. doi:10.1038/nmeth.1855

Schwartz, M. A. and Madhani, H. D. (2004). Principles of map kinase signaling specificity in *Saccharomyces cerevisiae*. *Annu. Rev. Genet.* **38**, 725-748. doi:10.1146/annurev.genet.39.073003.112634

Seger, R., Seger, D., Reszka, A. A., Munar, E. S., Eldar-Finkelman, H., Dobrowolska, G., Jensen, A. M., Campbell, J. S., Fischer, E. H. and Krebs, E. G. (1994). Overexpression of mitogen-activated protein kinase kinase (MAPKK) and its mutants in NIH 3T3 cells. Evidence that MAPKK involvement in cellular proliferation is regulated by phosphorylation of serine residues in its

kinase subdomains VII and VIII. *J. Biol. Chem.* **269**, 25699-25709. doi:10.1016/S0021-9258(18)47305-X

Shapiro, P. S., Vaisberg, E., Hunt, A. J., Tolwinski, N. S., Whalen, A. M., Mcintosh, J. R. and Ahn, N. G. (1998). Activation of the MKK/ERK pathway during somatic cell mitosis: direct interactions of active ERK with kinetochores and regulation of the mitotic 3F3/2 phosphoantigen. *J. Cell Biol.* **142**, 1533-1545. doi:10.1083/jcb.142.6.1533

Sharma, V. (2018). ImageJ plugin HyperStackReg V5.6 (Version v5.6), pp. Zenodo.

Shaul, Y. D. and Seger, R. (2006). ERK1c regulates Golgi fragmentation during mitosis. *J. Cell Biol.* **172**, 885-897. doi:10.1083/jcb.200509063

Shaul, Y. D. and Seger, R. (2007). The MEK/ERK cascade: from signaling specificity to diverse functions. *Biochim. Biophys. Acta (BBA) Mol. Cell Res.* **1773**, 1213-1226. doi:10.1016/j.bbamcr.2006.10.005

Sidorova, J. and Breeden, L. (1993). Analysis of the SWI4/SWI6 protein complex, which directs G1/S-specific transcription in Saccharomyces cerevisiae. *Mol. Cell. Biol.* **13**, 1069-1077.

Sikorski, R. S. and Hieter, P. (1989). A system of shuttle vectors and yeast host strains designed for efficient manipulation of DNA in *Saccharomyces cerevisiae*. *Genetics* **122**, 19-27. doi:10.1093/genetics/122.1.19

Slater, M. L. (1973). Effect of reversible inhibition of deoxyribonucleic acid synthesis on the yeast cell cycle. *J. Bacteriol.* **113**, 263-270. doi:10.1128/jb.113.1.263-270.1973

Slater, M. L. (1974). Recovery of yeast from transient inhibition of DNA synthesis. *Nature* **247**, 275-276. doi:10.1038/247275a0

Spellman, P. T., Sherlock, G., Zhang, M. Q., Iyer, V. R., Anders, K., Eisen, M. B., Brown, P. O., Botstein, D. and Futcher, B. (1998). Comprehensive identification of cell cycle-regulated genes of the yeast *Saccharomyces cerevisiae* by microarray hybridization. *Mol. Biol. Cell* **9**, 3273-3297. doi:10.1091/mbc.9.12.3273

Stevenson, B. J., Rhodes, N., Errede, B. and Sprague, G. F. (1992). Constitutive mutants of the protein kinase STE11 activate the yeast pheromone response pathway in the absence of the G protein. *Genes Dev.* **6**, 1293-1304. doi:10.1101/gad.6.7.1293

Strickfaden, S. C., Winters, M. J., Ben-Ari, G., Lamson, R. E., Tyers, M. and Pryciak, P. M. (2007). A mechanism for cell-cycle regulation of MAP kinase signaling in a yeast differentiation pathway. *Cell* **128**, 519-531. doi:10.1016/j.cell.2006.12.032

Taheri, N., Köhler, T., Braus, G. H. and Mösch, H.-U. (2000). Asymmetrically localized Bud8p and Bud9p proteins control yeast cell polarity and development. *EMBO J.* **19**, 6686-6696. doi:10.1093/emboj/19.24.6686

Tanaka, K., Tatebayashi, K., Nishimura, A., Yamamoto, K., Yang, H. Y. and Saito, H. (2014). Yeast osmosensors Hkr1 and Msb2 activate the Hog1 MAPK cascade by different mechanisms. *Sci. Signal.* **7**, ra21. doi:10.1126/scisignal.2004780

Tatebayashi, K., Yamamoto, K., Tanaka, K., Tomida, T., Maruoka, T., Kasukawa, E. and Saito, H. (2006). Adaptor functions of Cdc42, Ste50, and Sho1 in the yeast osmoregulatory HOG MAPK pathway. *EMBO J.* **25**, 3033-3044. doi:10.1038/sj.emboj.7601192

Tatebayashi, K., Tanaka, K., Yang, H.-Y., Yamamoto, K., Matsushita, Y., Tomida, T., Imai, M. and Saito, H. (2007). Transmembrane mucins Hkr1 and Msb2 are putative osmosensors in the SHO1 branch of yeast HOG pathway. *EMBO J.* **26**, 3521-3533. doi:10.1038/sj.emboj.7601796

Tatebayashi, K., Yamamoto, K., Nagoya, M., Takayama, T., Nishimura, A., Sakurai, M., Momma, T. and Saito, H. (2015). Osmosensing and scaffolding functions of the oligomeric four-transmembrane domain osmosensor Sho1. *Nat. Commun.* **6**, 6975. doi:10.1038/ncomms7975

Thévenaz, P., Ruttimann, U. E. and Unser, M. (1998). A pyramid approach to subpixel registration based on intensity. *IEEE Trans. Image Process.* **7**, 27-41. doi:10.1109/83.650848

Vadaie, N., Dionne, H., Akajagbor, D. S., Nickerson, S. R., Krysan, D. J. and Cullen, P. J. (2008). Cleavage of the signaling mucin Msb2 by the aspartyl protease Yps1 is required for MAPK activation in yeast. *J. Cell Biol.* **181**, 1073-1081. doi:10.1083/jcb.200704079

Vallen, E. A., Caviston, J. and Bi, E. (2000). Roles of Hof1p, Bni1p, Bnr1p, and myo1p in cytokinesis in *Saccharomyces cerevisiae*. *Mol. Biol. Cell* **11**, 593-611. doi:10.1091/mbc.11.2.593

Van Der Felden, J., Weisser, S., Brückner, S., Lenz, P. and Mösch, H.-U. (2014). The transcription factors Tec1 and Ste12 interact with Coregulators Msa1 and Msa2 To activate adhesion and multicellular development. *Mol. Cell. Biol.* **34**, 2283. doi:10.1128/MCB.01599-13

Vandermeulen, M. D. and Cullen, P. J. (2020). New aspects of invasive growth regulation identified by functional profiling of MAPK pathway targets in Saccharomyces cerevisiae. *Genetics* **216**, 95-116. doi:10.1534/genetics.120.303369

Vinod, P. K., Sengupta, N., Bhat, P. J. and Venkatesh, K. V. (2008). Integration of global signaling pathways, cAMP-PKA, MAPK and TOR in the regulation of FLO11. *PLoS ONE* **3**, e1663. doi:10.1371/journal.pone.0001663

Waltermann, C., Floettmann, M. and Klipp, E. (2010). G1 and G2 arrests in response to osmotic shock are robust properties of the budding yeast cell cycle. *Genome Inform.* **24**, 204-217. doi:10.1142/9781848166585_0017

White, M. A., Riles, L. and Cohen, B. A. (2009). A systematic screen for transcriptional regulators of the yeast cell cycle. *Genetics* **181**, 435-446. doi:10.1534/genetics.108.098145

Wilson, W. A., Hawley, S. A. and Hardie, D. G. (1996). Glucose repression/derepression in budding yeast: SNF1 protein kinase is activated by phosphorylation under derepressing conditions, and this correlates with a high AMP:ATP ratio. *Curr. Biol.* **6**, 1426-1434. doi:10.1016/S0960-9822(96)00747-6

Wittenberg, C. and Reed, S. I. (2005). Cell cycle-dependent transcription in yeast: promoters, transcription factors, and transcriptomes. *Oncogene* **24**, 2746-2755. doi:10.1038/sj.onc.1208606

Wright, J. H., Munar, E., Jameson, D. R., Andreassen, P. R., Margolis, R. L., Seger, R. and Krebs, E. G. (1999). Mitogen-activated protein kinase kinase activity is required for the G_2/M transition of the cell cycle in mammalian fibroblasts. *Proc. Natl. Acad. Sci. USA* **96**, 11335-11340. doi:10.1073/pnas.96.20.11335

Yamamoto, K., Tatebayashi, K. and Saito, H. (2016). Binding of the extracellular eight-cysteine motif of Opy2 to the putative osmosensor Msb2 is essential for activation of the yeast high-osmolarity glycerol pathway. *Mol. Cell. Biol.* **36**, 475-487. doi:10.1128/MCB.00853-15

Yang, H.-Y., Tatebayashi, K., Yamamoto, K. and Saito, H. (2009). Glycosylation defects activate filamentous growth Kss1 MAPK and inhibit osmoregulatory Hog1 MAPK. *EMBO J.* **28**, 1380-1391. doi:10.1038/emboj.2009.104

Yofe, I., Weill, U., Meurer, M., Chuartzman, S., Zalckvar, E., Goldman, O., Ben-Dor, S., Schütze, C., Wiedemann, N., Knop, M. et al. (2016). One library to make them all: streamlining the creation of yeast libraries via a SWAp-Tag strategy. *Nat. Methods* **13**, 371-378. doi:10.1038/nmeth.3795

Yoon, S. and Seger, R. (2006). The extracellular signal-regulated kinase: multiple substrates regulate diverse cellular functions. *Growth Factors* **24**, 21-44. doi:10.1080/02699050500284218

Zehorai, E., Yao, Z., Plotnikov, A. and Seger, R. (2010). The subcellular localization of MEK and ERK—a novel nuclear translocation signal (NTS) paves a way to the nucleus. *Mol. Cell. Endocrinol.* **314**, 213-220. doi:10.1016/j.mce.2009.04.008

Fig._S1

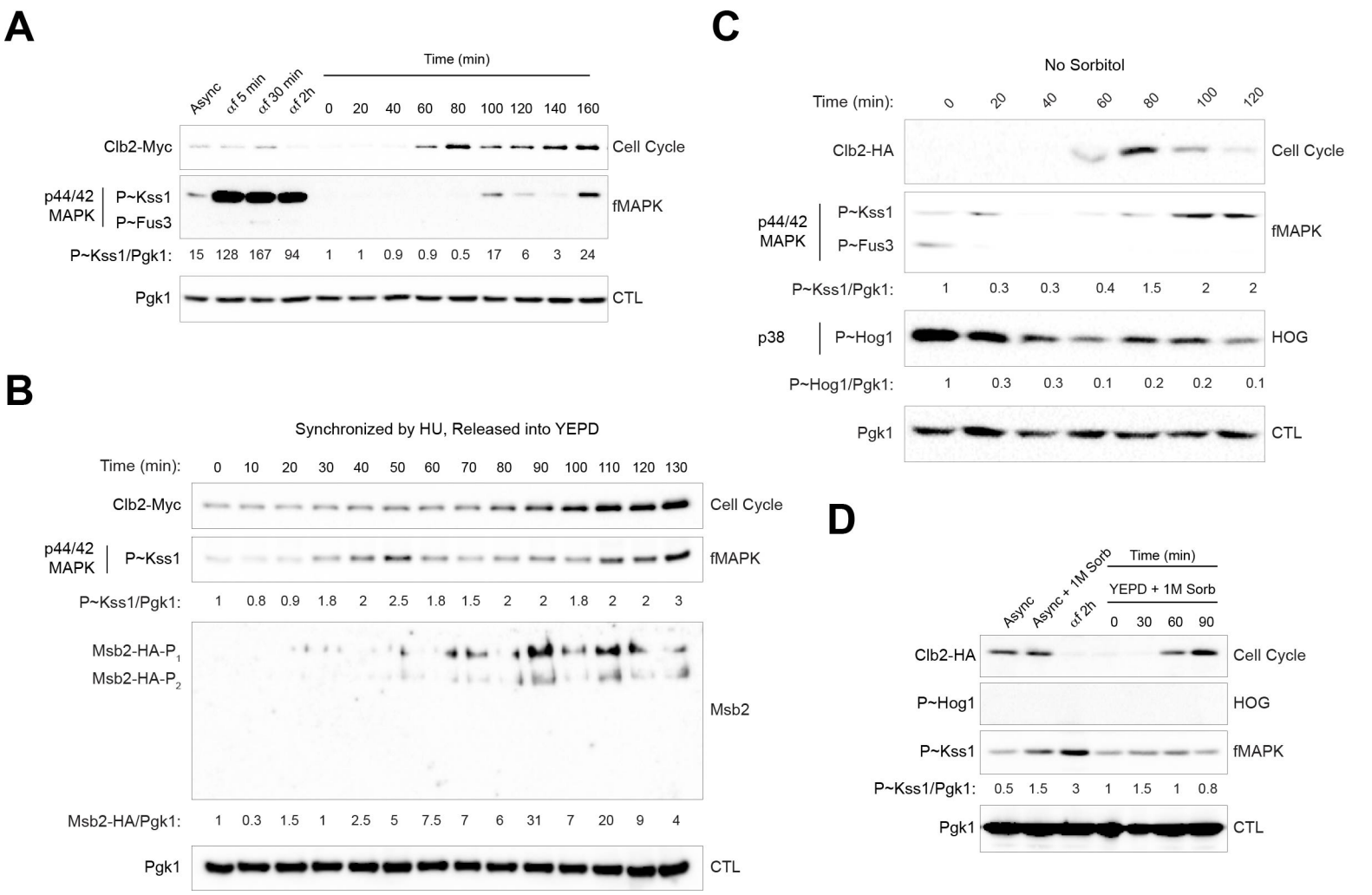

Fig. S1. Activity of the fMAPK pathway in hydroxyurea synchronized cells and of the HOG pathway in α-factor synchronized cells. (**A**) IB of wild type (PC7602 + p*STE4*) synchronized in G1 by α factor and released into YEPD medium. Samples were also harvested before (Async) and during α-factor (αf) treatment at indicated times. Cell extracts were probed with antibodies to Clb2p-Myc (to monitor the cell cycle), P~Kss1p (p44/42, to monitor fMAPK), and Pgk1p as a control for protein levels (CTL). Ratios of P~Kss1p to Pgk1p relative to time 0 (set to 1) are shown. (**B**) Immunoblot analysis of wild-type cells (PC7495) synchronized in S phase by hydroxyurea (HU) treatment. Cells were grown to (O.D.) A_{600} of 0.2 and incubated with 400 mM of HU for 4h. Arrested cells were washed and samples were harvested at the indicated times after release into YEPD medium. Cells extracts were probed with antibodies to Clb2p-Myc (cell cycle), P~Kss1p (p44/42, fMAPK), Msb2p-HA (Msb2), and Pgk1p, as a control for protein levels (CTL). Numbers refer to the ratio of P~Kss1p to Pgk1p levels and Msb2p-HA to Pgk1p levels relative to 0 min, which was set to 1. (**C**) Immunoblot analysis of wild-type cells (PC2744 + p*STE4*) synchronized in G_1 G1 by α-factor arrest. Samples were harvested at the indicated times after release into YEPD medium. Cell extracts were probed as in panel A and B. Numbers refer to the ratio of P~Kss1p to Pgk1p levels and P~Hog1p to Pgk1p levels relative to 0 min, which was set to 1. (**D**) IB analysis of the *pbs2*Δ (PC7493) mutant synchronized in G1. Synchronized cells were released into YEPD medium and at indicated times, resuspended in YEPD + 1M Sorb for 5 min before harvesting. Samples were also harvested before (Async) and during α-factor treatment (αf 2h). A sample of asynchronous culture was harvested and resuspended in YEPD supplemented with 1M sorbitol for 5 min (Async + 1M Sorb). Ratios of P~Kss1p to Pgk1p relative to time 0 (set to 1) are shown.

Fig._S2

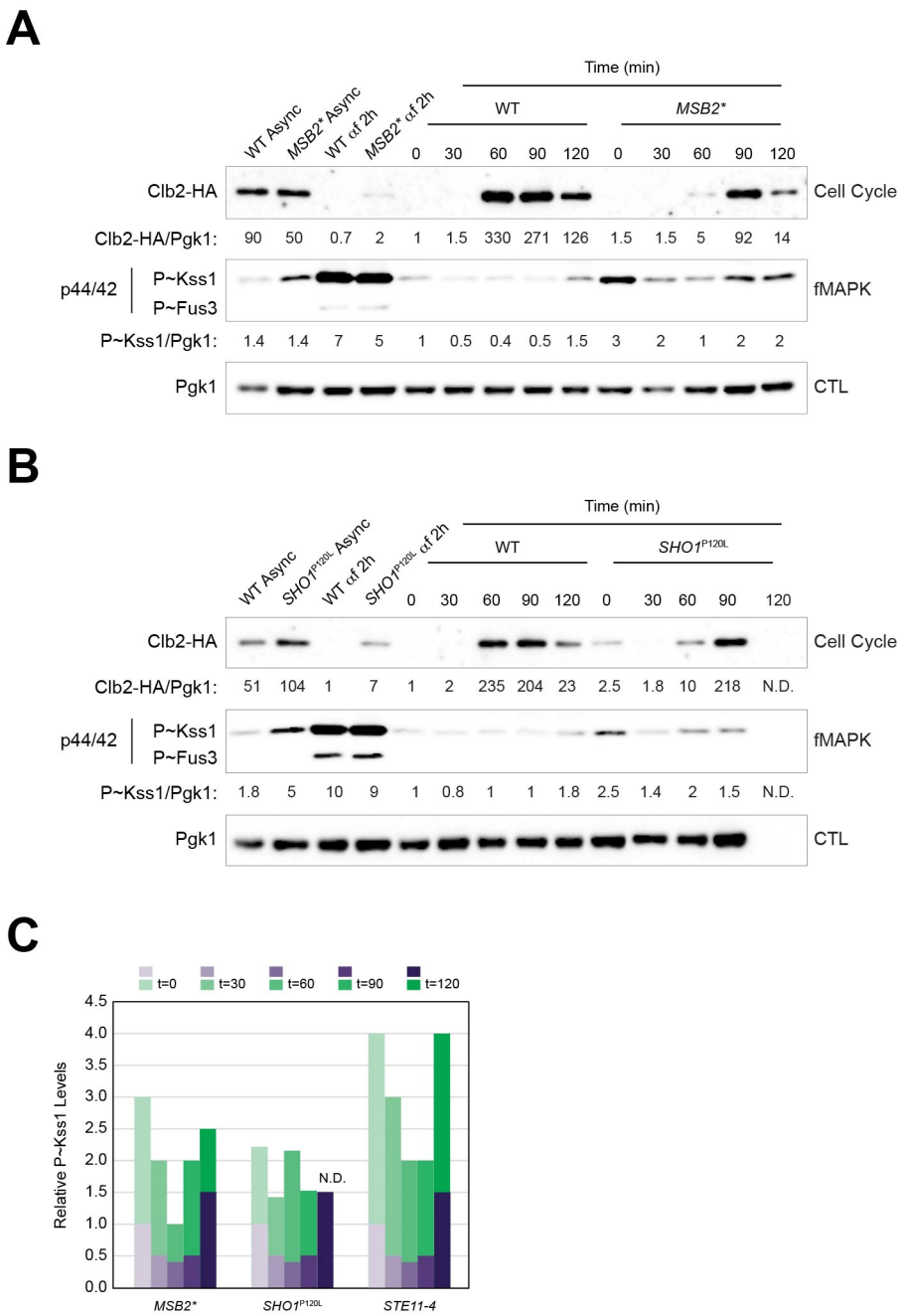

Fig. S2. **Cell-cycle pattern of fMAPK activity in different hyperactive alleles**. (**A**) Immunoblot analysis of synchronized cultures of wild type (PC7492) and *MSB2** (*GFP-MSB2*) strain (PC7492 + p*GFP-MSB2*) released in YEPD. See Figure 2A for details. Numbers refer to the ratio of Clb2p-HA to Pgk1p levels and P~Kss1p to Pgk1p levels relative to wild type at time 0, which was set to 1. The quantitation for WT Async and *MSB2** Async does not reflect the differences in P~Kss1p intensities. This may be due to the edge effects of the Pgk1p blot. WT, wild type. CTL, loading control. (**B**) Same as panel A, except wild type and *SHO1*^{P120L} strain (PC7492 + p*SHO1*^{P120L}). N.D, not determined. (**C**) Graphical representation of relative levels of P~Kss1p from panels A and B, and from Figure 2A. Purple, wild type; green, hyperactive alleles.

Fig._S3

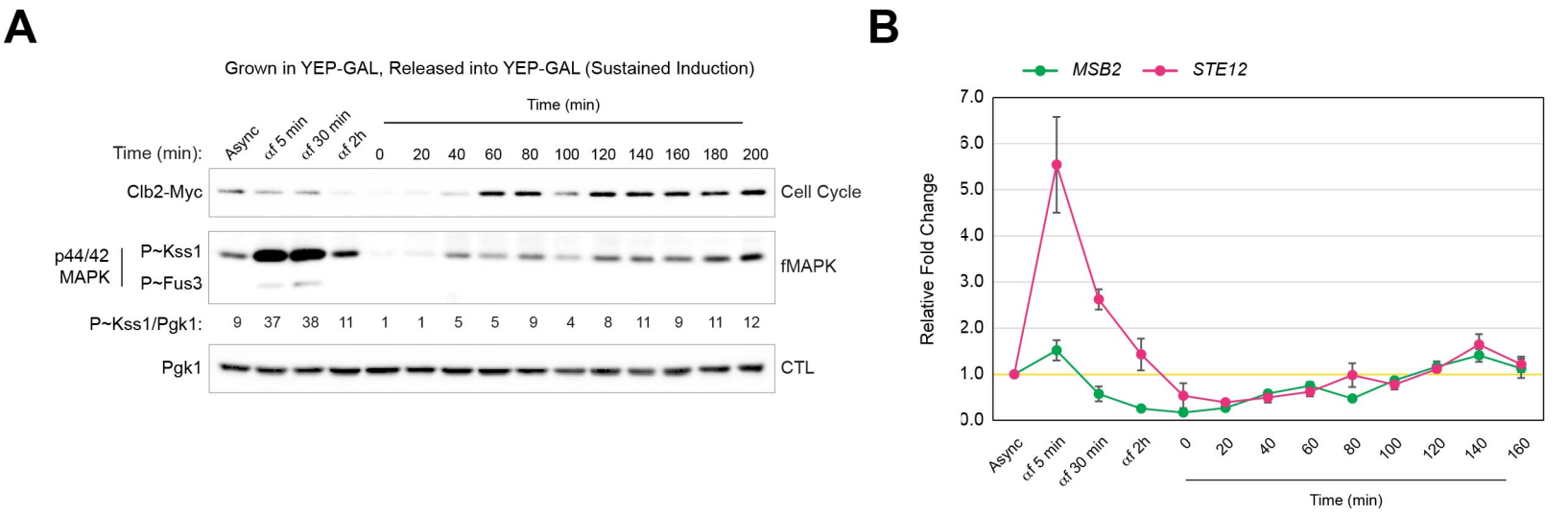

Fig. S3. Effect of pre-growth in GAL on fMAPK pathway activity throughout different phases of the cell cycle and expression profile of *STE12* and *MSB2* throughout the cell cycle. (**A**) Immunoblot analysis of wild-type cells (PC7602 + p*STE4*) pre-grown in YEP-GAL and synchronized in G_1 by α-factor arrest. Samples were harvested before (Async) and during α-factor treatment (αf 5 min, 30 min and 2 h) and at the indicated times after release into fresh YEP-GAL medium. Cell extracts were probed as in *Figure S1*. Numbers refer to the ratio of P~Kss1p to Pgk1p levels relative to 0 min, which was set to 1. **(B)** Fold changes in the mRNA levels of *MSB2* (green) and *STE12* (red) at indicated time points in synchronized cells relative to the asynchronous culture (Async). *MSB2* values were taken from **Fig. 2D**. See **Fig. 2D** for details. The fluctuations in *STE12* mRNA levels at αf = 5 min and at αf = 30 min were different from other time points.

Fig._S4

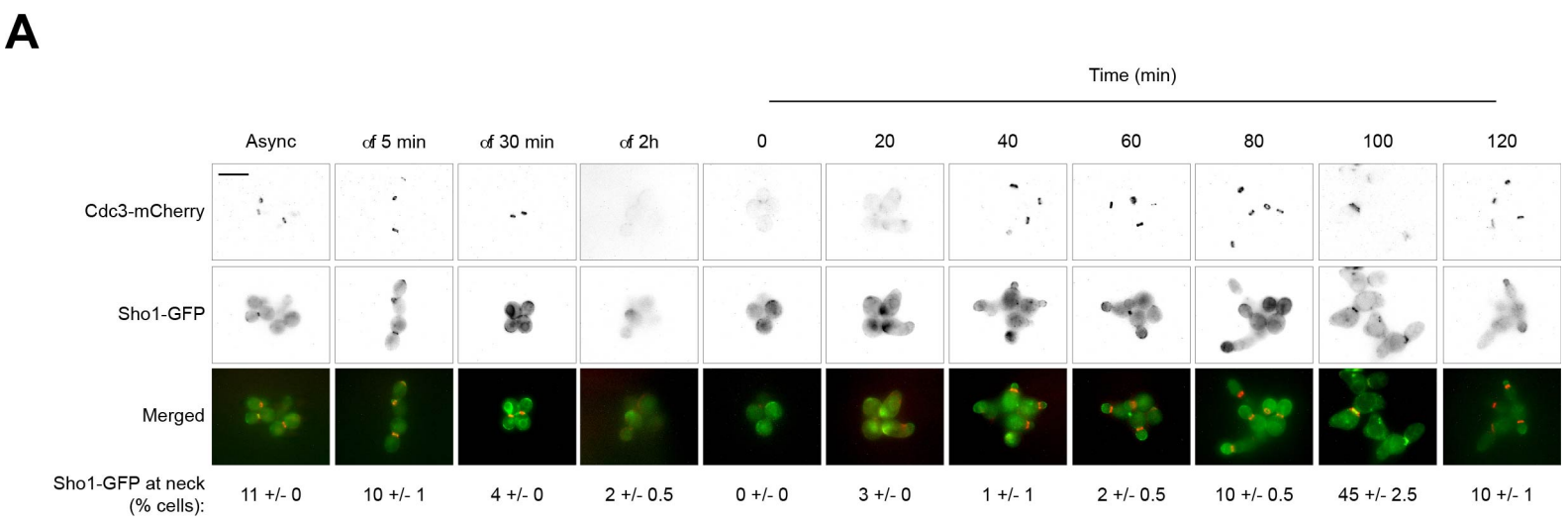

Fig. S4. Localization of Sho1p throughout the cell cycle and monitoring P~Kss1p using indirect immunofluorescence. (**A**) Inverted grayscale and merged images of maximum intensity projections of wild-type cells carrying Sho1p-GFP and Cdc3p-mCherry (PC7604 + p*SHO1-GFP*) harvested at indicated time from α-factor synchronized cells released into YEPD medium. Cdc3p-mCherry was used as a marker for cell-cycle progression. Numbers refer to number of cells showing Sho1p-GFP at the mother-bud-neck as percent of total cells. Error refers to S.E.M from 2 independent trials. Scale, 10 microns. (**B**) Indirect immunofluorescence of *slt2*Δ cells grown in YEP-GAL. Representative cells in different stages of growth are shown. See Fig. 5 for details. Numbers refer to normalized pixel intensity of P~Kss1p puncta in each cell. Error represents S.E.M among 20 cells. One-way ANOVA with Tukey's test was used for statistical analysis. Asterisk, intensity values for mitosis and post-mitosis cells are significantly different (p-value< 0.05) from other stages.

Fig._S5

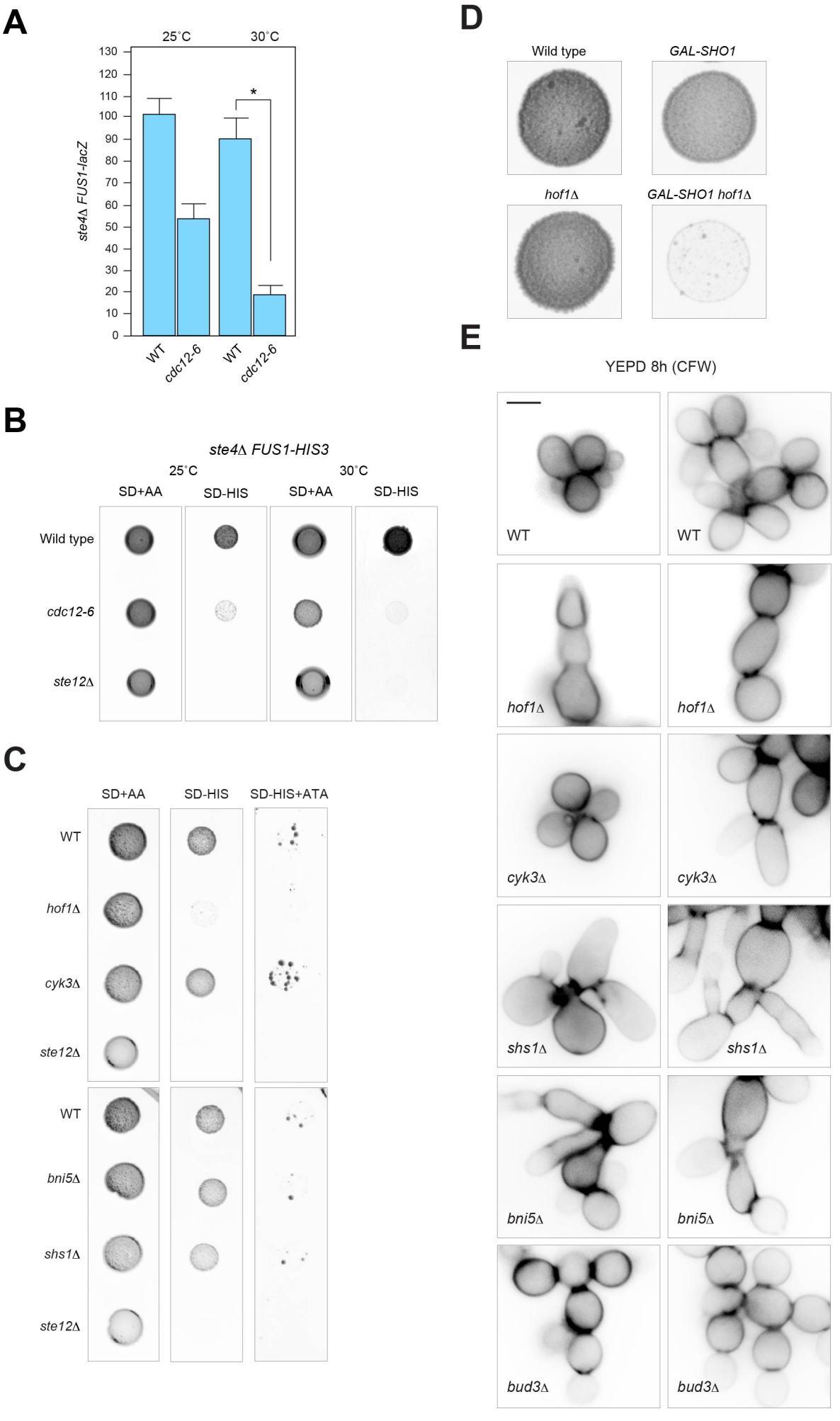

Fig. S5. fMAPK pathway activity and budding pattern of mutants lacking proteins that function in cytokinesis. (**A**) β-galactosidase assays of wild type (PC538), *cdc12-6* (PC2710), and *ste12*Δ (PC539) strains evaluated for *FUS1-lacZ* reporter activity. Cells were grown to mid-log state at indicated temperatures. Error bars represent the S.E.M. (n=3). **(B)** Wild type (PC538), *cdc12-6* (PC2710), and the *ste12*Δ mutant (PC539) evaluated for fMAPK activity using *FUS1-HIS3* growth reporter. Equal concentrations of cells were spotted onto SD+AA, SD-HIS, and SD-HIS+ATA media. Plates were incubated for 3 d at the indicated temperatures. (**C**) Activity of the *FUS1-HIS3* growth reporter for wild type (PC538), *hof1*Δ (PC2371), *cyk3*Δ (PC6472), *bni5*Δ (PC6475), *shs1*Δ (PC6476) and *ste12*Δ (PC539). See panel A for details. (**D**) Wild-type cells (PC538), *GAL-SHO1* (PC538 + p*GAL-SHO1*), *hof1*Δ (PC2371), and the *GAL-SHO1 hof1*Δ double mutant (PC2371 + p*GAL-SHO1*) were grown in GAL to evaluate genetic interaction between Hof1p and Sho1p. (**E**) Chitin staining of wild-type cells, and the *hof1*Δ, *cyk3*Δ, *shs1*Δ, *bni5*Δ, and *bud3*Δ (PC3635) mutants. Cells were incubated at low concentrations (0.01 O.D. at A_{600}) in YEPD media at 30˚C for 8 h. Cells were fixed in 13% formaldehyde and stained with fluorescent brightener #28 (Calcofluor white) at a concentration of 0.01% for 15 min. Duplicate examples are shown for each strain. Scale bar, 5 microns. WT, wild type.

Fig._S6

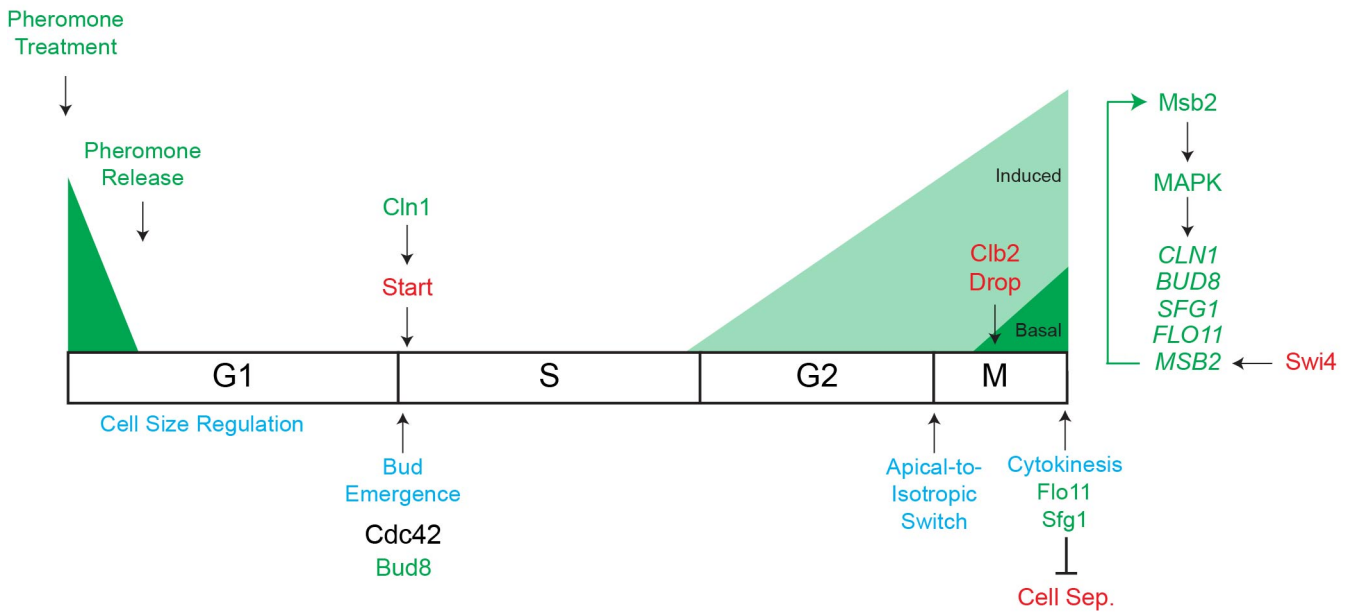

Fig. S6. Model for fMAPK activity over the cell cycle. The fMAPK activity increases in response to pheromone treatment. The drop in fMAPK activity occurs once the pheromone is washed away and arrested cells are allowed to progress through the cell cycle. The fMAPK activity then increases at the end of the cell cycle, in M/G1 under basal conditions (dark green), and in G2 under pathway-inducing conditions (light green). Cell cycle events are shown in blue and red. Genes written in green are direct targets of the fMAPK pathway and their protein products are mentioned in the appropriate stage of the cell cycle with an arrow. Cdc42p, the regulator of cell growth, polarity, and fMAPK pathway signaling, is shown in black.

Table S1. Yeast strains used in the study.

Name	Genotype	Reference
PC313	MATa *ura3-52*	(Liu et al. 1993)
PC538	MATa *ste4 FUS1-lacZ FUS1-HIS3 ura3-52*	(Cullen et al. 2004)
PC539	MATa *ste4 FUS1-lacZ FUS1-HIS3 ura3-52 ste12::URA3*	(Cullen et al. 2004)
PC546	MATa *ste4 FUS1-lacZ FUS1-HIS3 ura3-52 pbs2::KlURA3*	(Cullen et al. 2004)
PC611	MATa *ste4 FUS1-lacZ FUS1-HIS3 ura3-52 ste11::KlURA3*	(Cullen et al. 2004)
PC622	MATa *ste4 FUS1-lacZ FUS1-HIS3 ura3-52 GAL-SHO1::KanMX6*	(Cullen et al. 2004)
PC546	MATa *ste4 FUS1-lacZ FUS1-HIS3 ura3-52 pbs2::URA3*	(CULLEN AND SPRAGUE 2000)
PC644	MATa *ste4 FUS1-lacZ FUS1-HIS3 ura3-52 pbs2::ura3⁻*	This study
PC646	MATa *ste4 FUS1-lacZ FUS1-HIS3 ura3-52 pbs2::ura3⁻ ste12::URA3*	This study
PC947	MATa *ste4 FUS1-lacZ FUS1-HIS3 ura3-52 GAL-MSB2::KanMX6*	(CULLEN *et al.* 2004)
PC999	*MAT***a** *ste4 FUS1-lacZ FUS1-HIS3 ura3-52 MSB2-HA@500 aa*	(Cullen et al. 2004)
PC1052	MATa *ste4 FUS1-lacZ FUS1-HIS3 ura3-52 GAL-SHO1::KanMX6 ste11::KlURA3*	(PRABHAKAR *et al.* 2020)
PC1516	MATa *ste4 FUS1-lacZ FUS1-HIS3 ura3-52 MSB2-HA$^{\Delta 100\text{-}818}$*	(Cullen et al. 2004)
PC1531	MATa *ste4 FUS1-lacZ FUS1-HIS3 ura3-52 sho1::HYG*	(CULLEN *et al.* 2004)
PC1549	MATa *ste4 FUS1-lacZ FUS1-HIS3 ura3-52 SHO1-YFP::KanMX6*	(ADHIKARI *et al.* 2015a)
PC1806	MATa *ste4 FUS1-lacZ FUS1-HIS3 ura3-52 GAL-MSB2-HA$^{\Delta 100\text{-}818}$::KanMX6*	(PRABHAKAR *et al.* 2020)
PC1811	MATa *ste4 FUS1-lacZ FUS1-HIS3 ura3-52 MSB2-HA$^{\Delta 100\text{-}818}$ ste12::KlURA3*	(Vadaie et al. 2008)
PC1837	MATa *ste4 FUS1-lacZ FUS1-HIS3 ura3-52 GAL-MSB2-HA$^{\Delta 100\text{-}818}$::KanMX6 ste12::KlURA3*	(PRABHAKAR *et al.* 2020)
PC1839	MATa *ste4 FUS1-lacZ FUS1-HIS3 ura3-52 GAL-MSB2::NAT GAL-SHO1::HYG*	This study
PC2061	MATa *ste4 FUS1-lacZ FUS1-HIS3 ura3-52 ssk1::NAT ste11::KlURA3*	(PITONIAK *et al.* 2009)
PC2371	MATa *ste4 FUS1-lacZ FUS1-HIS3 ura3-52 hof1::KlURA3*	This study
PC2372	MATa *ste4 FUS1-lacZ FUS1-HIS3 ura3-52 GAL-SHO1::KanMX6 hof1::KlURA3*	This study
PC2377	MATa *ste4 FUS1-lacZ FUS1-HIS3 ura3-52 SHO1-YFP::KanMX6 HOF1-CFP::HYG*	This study
PC2710	MATa *ste4 FUS1-lacZ FUS1-HIS3 ura3-52 cdc12-6::NAT*	(Basu et al. 2016)
PC2744	MATa *ste4 FUS1-lacZ FUS1-HIS3 ura3-52 CLB2-HA*	(PRABHAKAR *et al.* 2020)
PC3394	*MAT***a** *ste4 FUS1-lacZ FUS1-HIS3 ura3-52 MSB2-HA@500 aa slt2*	(BIRKAYA *et al.* 2009)
PC3428	*MAT***a** *ste4 FUS1-lacZ FUS1-HIS3 ura3-52 MSB2-HA@500 aa swi4::KlURA3*	(CHAVEL *et al.* 2010)
PC3635	MATa *ste4 FUS1-lacZ FUS1-HIS3 ura3-52 bud3::KlURA3*	(BASU *et al.* 2016)
PC6472	MATa *ste4 FUS1-lacZ FUS1-HIS3 ura3-52 cyk3::KlURA3*	(BASU *et al.* 2020)
PC6475	MATa *ste4 FUS1-lacZ FUS1-HIS3 ura3-52 bni5::KlURA3*	This study
PC6476	MATa *ste4 FUS1-lacZ FUS1-HIS3 ura3-52 shs1::KlURA3*	This study
PC6591	*MAT***a** *ura3-52 leu2*	(BASU *et al.* 2020)
PC6810	*MAT***a** *ura3-52 leu2 ssk1*	(Basu et al. 2020)
PC7365	MATa *ura3-52 CDC3-mCherry::HYG*	(PRABHAKAR *et al.* 2020)
PC7492	*MAT***a** *ura3-52 leu2 CLB2-HA:: KanMX6*	This study
PC7493	*MAT***a** *ura3-52 leu2 CLB2-HA:: KanMX6 pbs2::NAT*	This study
PC7494	*MAT***a** *ura3-52 leu2 ssk1 CLB2-HA:: KanMX6*	This study
PC7495	*MAT***a** *ste4 FUS1-lacZ FUS1-HIS3 ura3-52 MSB2-HA@500 aa CLB2-MYC:: KanMX6*	This study
PC7563	MATa *ura3-52 CDC3-mCherry::HYG hof1::NAT*	This study
PC7602	MATa *ste4 FUS1-lacZ FUS1-HIS3 ura3-52 HKR1-HA@895 bp CLB2-MYC:: KanMX6*	This study
PC7604	MATa *ura3-52 CDC3-mCherry::HYG CLB2-MYC::KanMX6*	This study
PC7626	*MAT***a** *ura3-52 leu2 ssk1 swi4::NAT*	This study
PC7658	*MAT***a** *ste4 FUS1-lacZ FUS1-HIS3 ura3-52 MSB2-HA@500 aa CLB2-MYC:: KanMX6 swi4::NAT*	This study

a. All strains are Σ1278b background unless otherwise indicated.

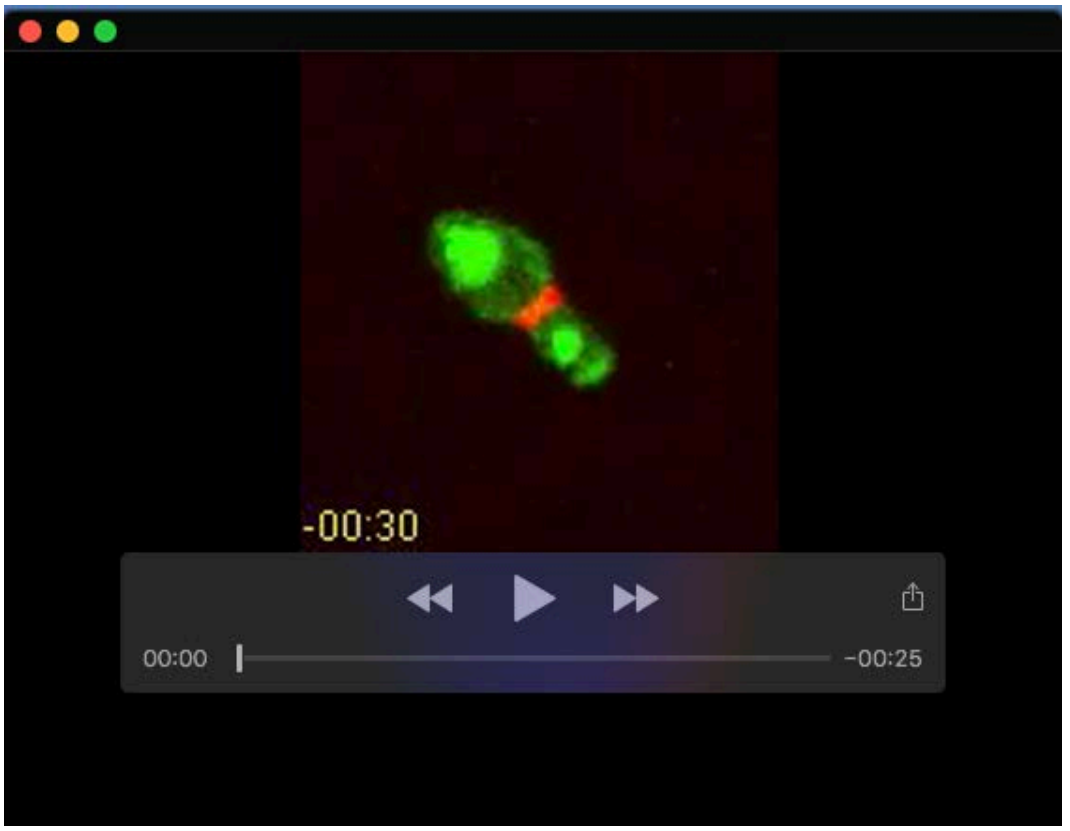

Movie 1. Time lapse of *GAL-GFP-MSB2* cells expressing Cdc3p-mCherry (PC7365 + p*GAL-GFP-MSB2*) in GAL. Time interval, 10 min. Time 0 is when septin hourglass splits into a double ring marking cytokinesis. Scale bar, 5 microns.

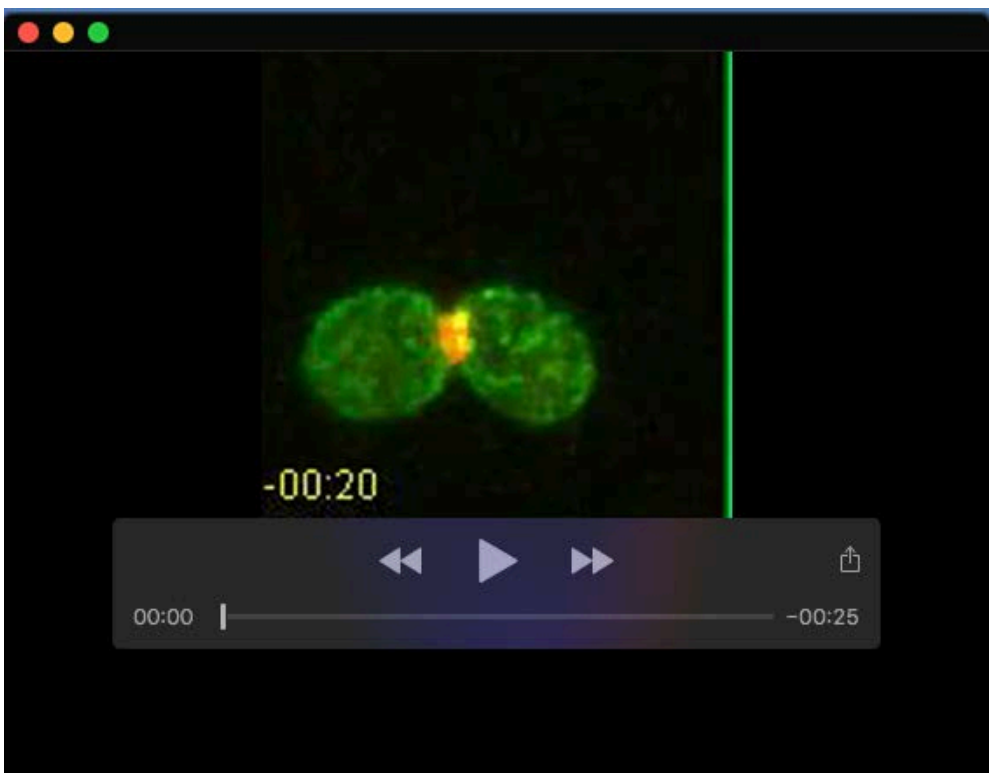

Movie 2. Time lapse movie showing of wild-type cells expressing Cdc3p-mCherry and Sho1p-GFP (PC7365 + p*SHO1-GFP*) in GLU. See movie 1 for details. Blue arrowhead, septin split into a double ring marks cytokinesis; red arrow, Sho1p-GFP localizing to the presumptive bud sites; black arrow, Sho1p-GFP localizing to the neck when septin split into a double ring. Scale bar, 5 microns.

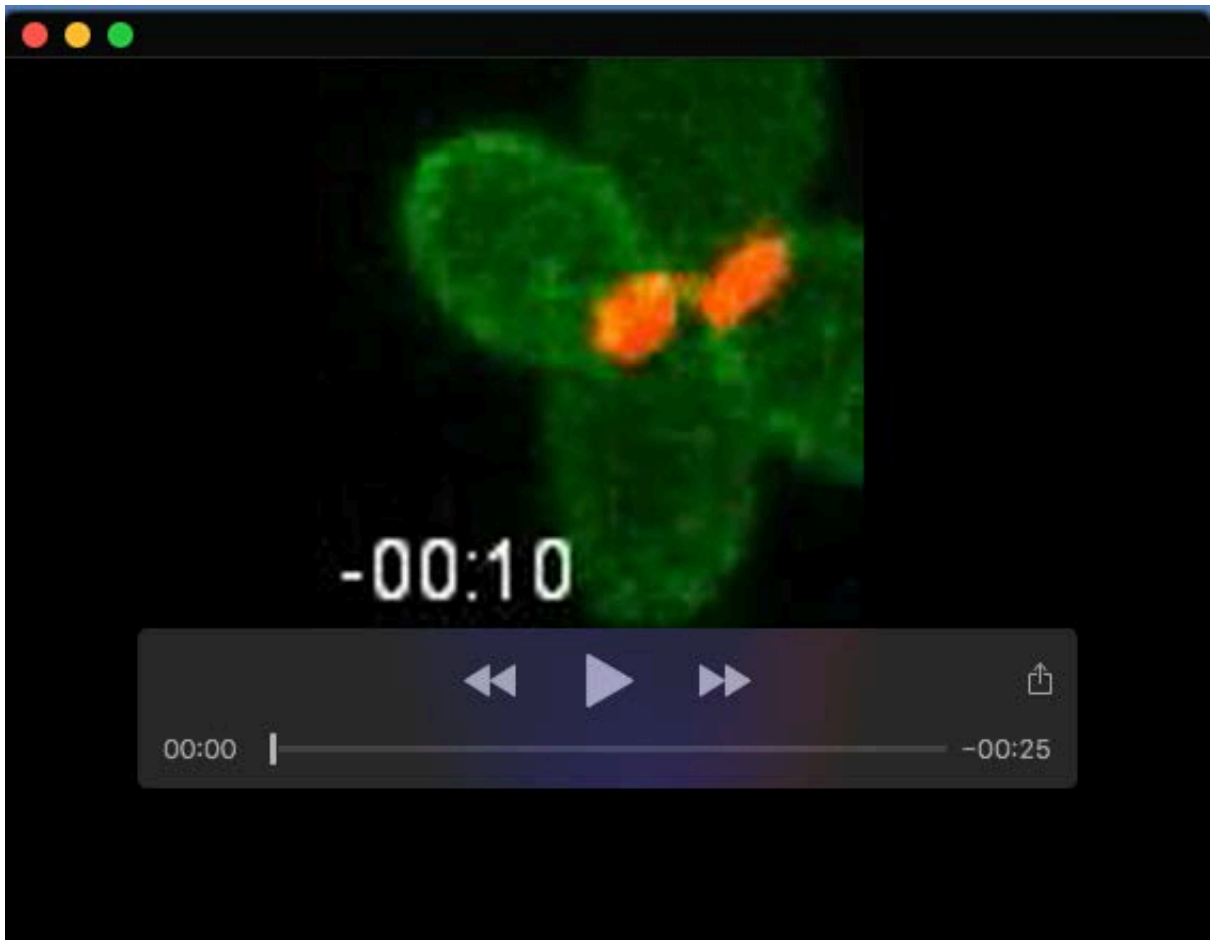

Movie 3. Second example of wild-type cells expressing Cdc3p-mCherry and Sho1p-GFP (PC7365 + p*SHO1-GFP*) in GLU. See movie 2 for details.

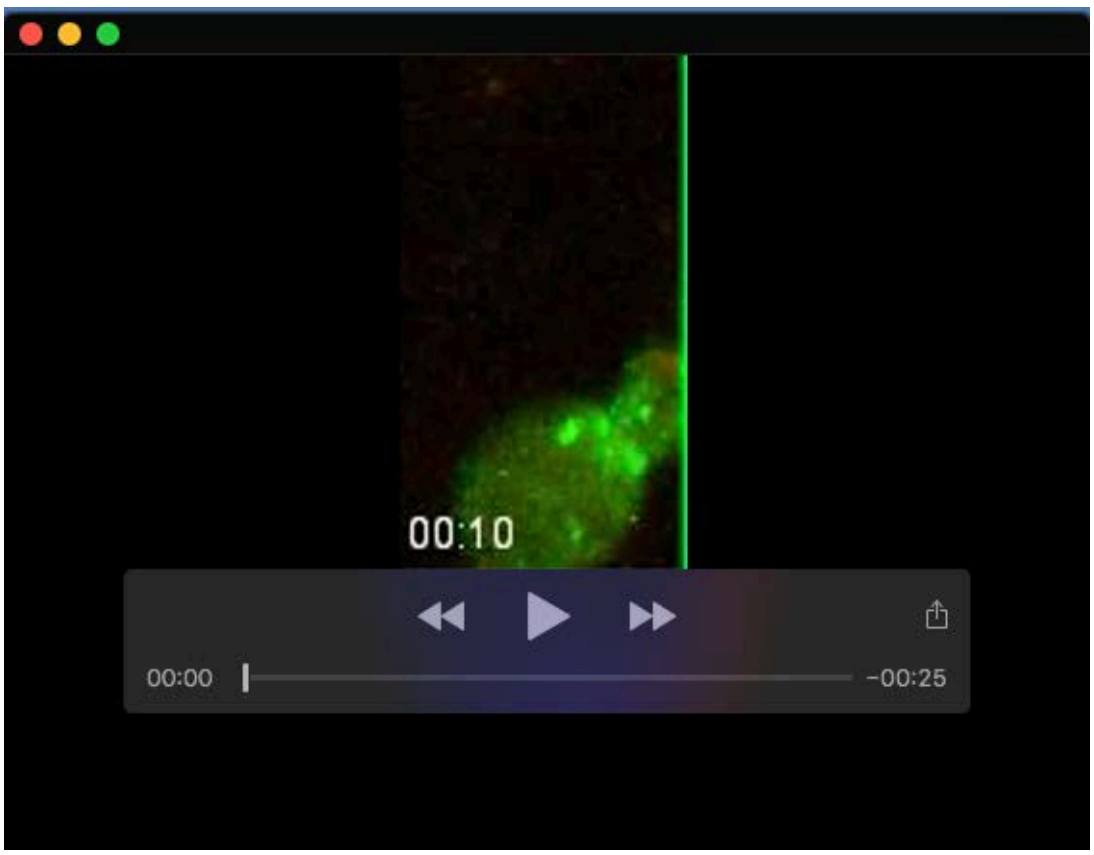

Movie 4. Time lapse movie of wild-type cells expressing Cdc3p-mCherry and Sho1p-GFP (PC7365 + p*SHO1-GFP*) in GAL. See movie 2 for details. Time 0 indicates start of experiment.

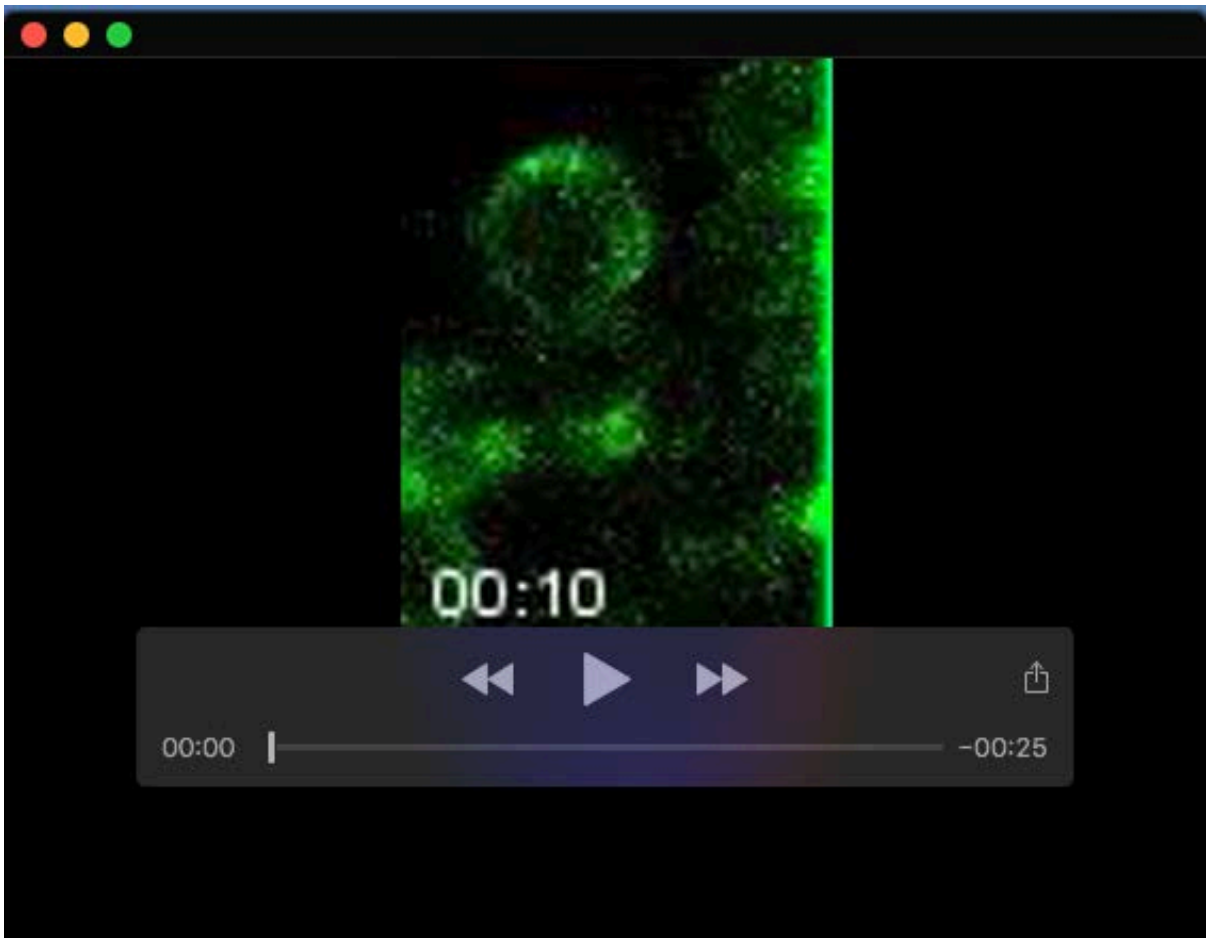

Movie 5. Time lapse movie showing the co-localization of Hof1p-CFP and Sho1p-YFP in wild-type cells (PC2377). Colors of fluorescence proteins were change to red (Hof1p-CFP) and green (Sho1p-YFP) in the merged channel for better visualization. Red arrows, localization of Hof1p-CFP at the neck; green arrows, localization of Sho1p-YFP at the neck. Time 0 indicates start of experiment. Scale bar, 5 microns.

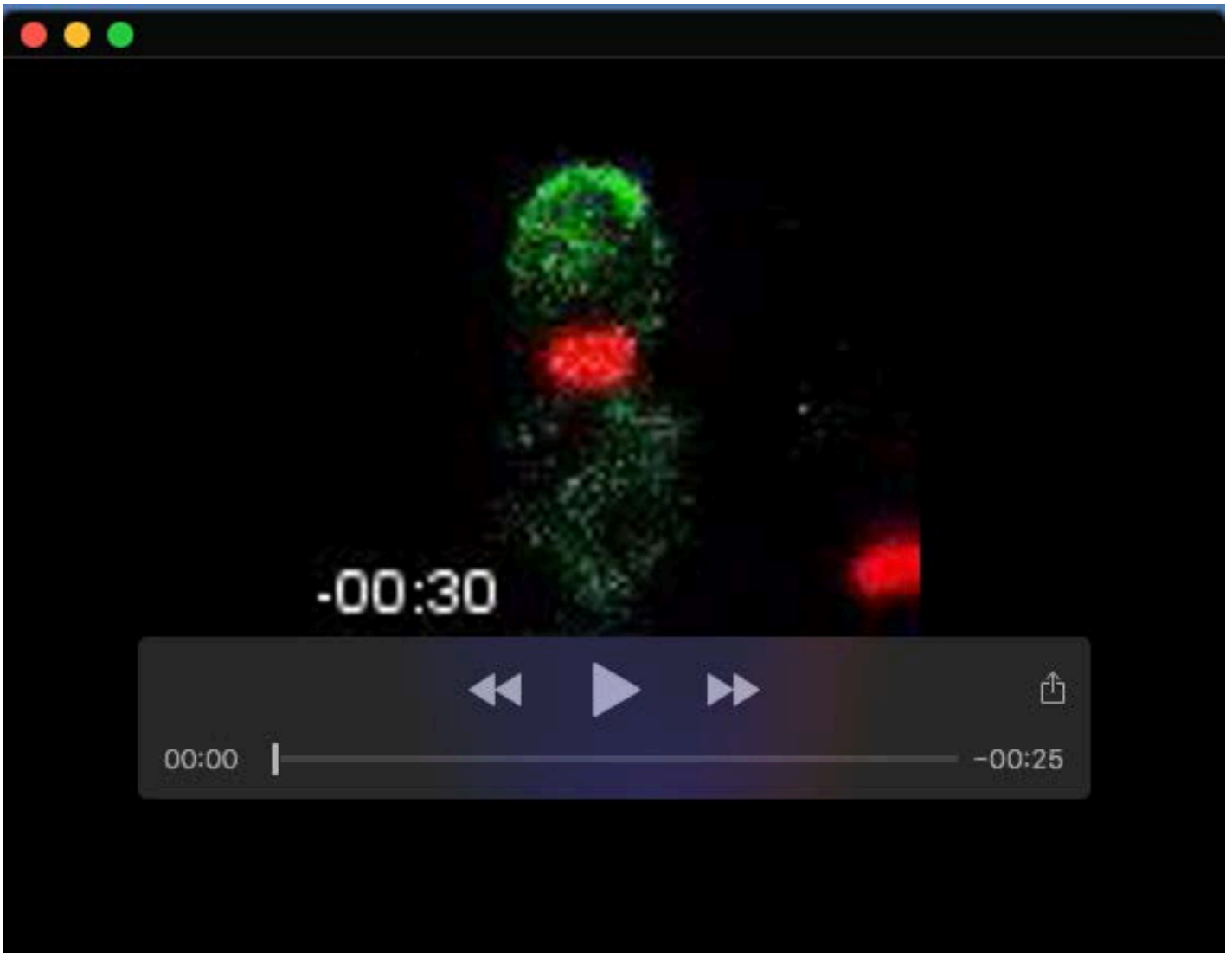

Movie 6. Time lapse movie showing the co-localization of Sho1p-GFP and Cdc3p-mCherry in the *hof1*Δ mutant (PC7563 + p*SHO1-GFP*). See movie 2 for details. An example of normal localization of Sho1p-GFP, which is seen in 90% of cells. Scale bar, 10 microns.

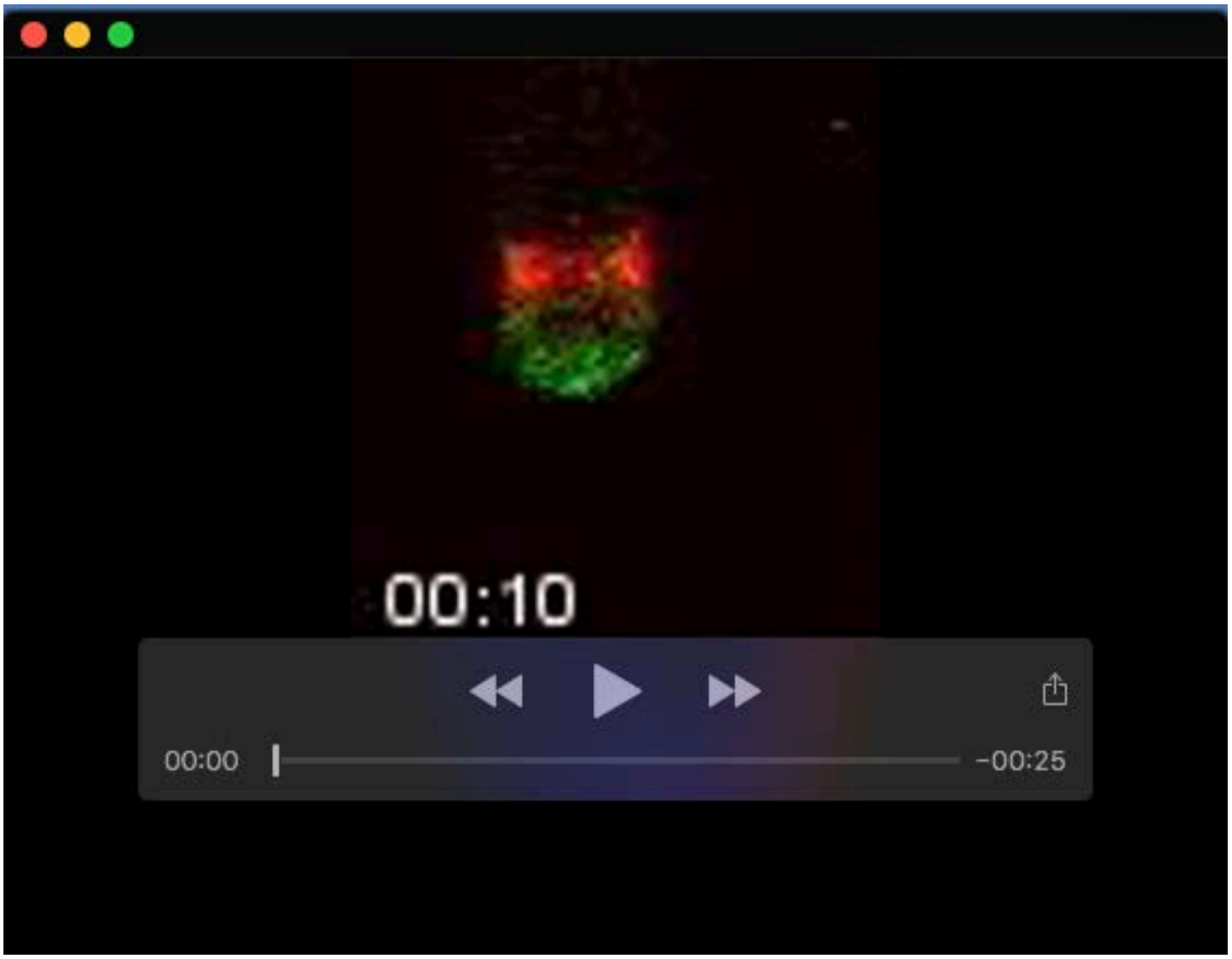

Movie 7. Time lapse movie showing the co-localization of Sho1p-GFP and Cdc3p-mCherry in the *hof1*Δ mutant. See movie 2 for details. An example of Sho1p-GFP mis-localization, which is seen in 10% of cells. Scale bar, 5 microns.